# Aerosol-water interaction at sub and super-saturated regimes

## From small scale molecular mechanisms to large scale atmospheric models

**Narges Rastak**

Academic dissertation for the Degree of Doctor of Philosophy in Environmental Sciences at Stockholm University to be publicly defended on Friday 25 May 2018 at 10.00 in Ahlmannsalen,Geovetenskapens hus, Svante Arrhenius väg 12.

**Abstract**

The term "atmospheric aerosol" refers to solid or liquid particles suspended in the atmosphere. Atmospheric aerosols influence the Earth's energy budget directly by scattering and absorbing radiation (known as the direct aerosol effect) and indirectly by acting as cloud condensation nuclei (CCN) and ice nucleating particles and thereby modifying cloud properties (known as the indirect aerosol effect). The water-affinity of aerosols plays an important role on one hand in defining the aerosol water-content and optical properties, and on the other hand in determining the conditions at which the aerosols can act as CCN. Aerosol-water interactions thus affect both the direct as well as the indirect aerosol effects, leading to impacts on the Earth's energy budget and ultimately climate. The role of aerosols and clouds in determining the radiative balance of the Earth is one of the largest sources of uncertainty in understanding climate change. Therefore, the main goal of this thesis was to improve the knowledge of aerosol-water interactions. In this thesis, we investigated the links between aerosol molecular composition, hygroscopic growth and CCN activation, with a focus on organic compounds. Specifically, we tested several commonly-used simplifying approaches for describing water uptake, CCN activation and their impact on aerosol radiative properties.

The traditional Köhler theory that describes the equilibrium between droplet and vapor phase along with modifications of these theory were used to investigate the water affinity of aerosol particles. The modifications to this theory used in this study are as follows: complete dissolution, hygroscopicity parameter (κ), soluble fraction (ε), treatment of adsorption, counting for gas-particle partitioning of volatile organic compounds. Also a Solubility Basis Set (SBS) model was developed to investigate the CCN activation behavior of complex organic aerosols accounting for the distribution of solubilities present in these mixtures. Based on the theoretical approaches, a coupled hygroscopicity and radiative transfer model was developed to investigate the effect of hygroscopic growth and CCN activation of aerosol particles on radiative properties in Arctic and boreal forest environments. Finally on the global scale, we used two climate models (NorESM and ECHAM6-HAM2) to investigate the sensitivity of climate models to treatment of water uptake of organics.

By using different thermodynamic modelling approaches it was found that an approach using assumptions of limited solubility of the SOA components and solubility distributions cannot alone explain the hygroscopic behavior of SOA at subsaturation, while they can explain the CCN activation behaviour of organic mixtures. Quantifying the hygroscopic behavior of SOA compounds below 90% Relative Humidity (RH) requires consideration of processes such as adsorptive water uptake, bulk to surface partitioning, gas-particle partitioning of the semivolatile vapors and non ideality of the liquid phases with decreasing relative humidity (RH). On the other hand, at supersaturation most SOA behave as nearly completely soluble in water. We found that the differences in water-affinity of SOA at sub- and supersaturated conditions can be explained by Liquid-Liquid Phase Separation (LLPS) effects. By using the coupled hygroscopicity and radiative transfer model, a great impact of water uptake of aerosol particles on direct radiative effect was found in Arctic and boreal forest environment. The climate impacts resulting from OA are currently estimated using model parameterizations of water uptake that drastically simplify this complexity of OA. We found that the single-parameter hygroscopicity framework commonly used in climate models, can introduce significant errors when quantifying the climate effects of OA. The results highlight the need for better constraints on the interactions between water vapor and OA and its molecular composition, as well as overall global OA mass loadings, including currently under-explored anthropogenic and marine OA sources.

Stockholm 2018
http://urn.kb.se/resolve?urn=urn:nbn:se:su:diva-154856

ISBN 978-91-7797-282-2
ISBN 978-91-7797-283-9

**Department of Environmental Science and Analytical Chemistry**

Stockholm University, 106 91 Stockholm

# AEROSOL-WATER INTERACTION AT SUB AND SUPER-SATURATED REGIMES

Narges Rastak

Stockholm University

# Aerosol-water interaction at sub and super-saturated regimes

From small scale molecular mechanisms to large scale atmospheric models

Narges Rastak

ISBN print 978-91-7797-282-2
ISBN PDF 978-91-7797-283-9

Printed in Sweden by US-AB, Stockholm 2018
Distributor: Department of Environmental Science and Analytical Chemistry (ACES), Stockholm University

# Abstract

The term “atmospheric aerosol” refers to solid or liquid particles suspended in the atmosphere. Atmospheric aerosols influence the Earth’s energy budget directly by scattering and absorbing radiation (known as the direct aerosol effect) and indirectly by acting as cloud condensation nuclei (CCN) and ice nucleating particles and thereby modifying cloud properties (known as the indirect aerosol effect). The water-affinity of aerosols plays an important role on one hand in defining the aerosol water-content and optical properties, and on the other hand in determining the conditions at which the aerosols can act as CCN. Aerosol-water interactions thus affect both the direct as well as the indirect aerosol effects, leading to impacts on the Earth’s energy budget and ultimately climate. The role of aerosols and clouds in determining the radiative balance of the Earth is one of the largest sources of uncertainty in understanding climate change. Therefore, the main goal of this thesis was to improve the knowledge of aerosol-water interactions. In this thesis, we investigated the links between aerosol molecular composition, hygroscopic growth and CCN activation, with a focus on organic compounds. Specifically, we tested several commonly-used simplifying approaches for describing water uptake, CCN activation and their impact on aerosol radiative properties.

The traditional Köhler theory that describes the equilibrium between droplet and vapor phase along with modifications of these theory were used to investigate the water affinity of aerosol particles. The modifications to this theory used in this study are as follows: complete dissolution, hygroscopicity parameter ($\kappa$), soluble fraction ($\varepsilon$), treatment of adsorption, counting for gas-particle partitioning of volatile organic compounds. Also a Solubility Basis Set (SBS) model was developed to investigate the CCN activation behavior of complex organic aerosols accounting for the distribution of solubilities present in these mixtures. Based on the theoretical approaches, a coupled hygroscopicity and radiative transfer model was developed to investigate the effect of hygroscopic growth and CCN activation of aerosol particles on radiative properties in Arctic and boreal forest environments. Finally on the global scale, we used two climate models (NorESM and ECHAM6-HAM2) to investigate the sensitivity of climate models to treatment of water uptake of organics.

By using different thermodynamic modelling approaches it was found that an approach using assumptions of limited solubility of the SOA components and solubility distributions cannot alone explain the hygroscopic behavior of

SOA at subsaturation, while they can explain the CCN activation behaviour of organic mixtures. Quantifying the hygroscopic behavior of SOA compounds below 90% Relative Humidity (RH) requires consideration of processes such as adsorptive water uptake, bulk to surface partitioning, gas-particle partitioning of the semivolatile vapors and non ideality of the liquid phases with decreasing relative humidity (RH). On the other hand, at supersaturation most SOA behave as nearly completely soluble in water. We found that the differences in water-affinity of SOA at sub- and supersaturated conditions can be explained by Liquid-Liquid Phase Separation (LLPS) effects. By using the coupled hygroscopicity and radiative transfer model, a great impact of water uptake of aerosol particles on direct radiative effect was found in Arctic and boreal forest environment. The climate impacts resulting from OA are currently estimated using model parameterizations of water uptake that drastically simplify this complexity of OA. We found that the single-parameter hygroscopicity framework commonly used in climate models, can introduce significant errors when quantifying the climate effects of OA. The results highlight the need for better constraints on the interactions between water vapor and OA and its molecular composition, as well as overall global OA mass loadings, including currently under-explored anthropogenic and marine OA sources.

# Sammanfattning

Termen "atmosfärisk aerosol" avser fasta eller flytande partiklar suspenderade i atmosfären. Atmosfäriska aerosoler påverkar jordens energibudget direkt genom att sprida och absorbera strålning ( den direkta aerosol-effekten) och indirekt genom att fungera som molnkondensationskärnor (CCN) och iskärnbildande partiklar och därmed modifiera molnens egenskaper (den indirekta aerosol-effekten). Hygroskopiciteten hos aerosoler spelar å ena sidan en viktig roll för hur mycket vatten aerosolen tar upp i undermättade miljöer och därmed de optiska egenskaperna och å andra sidan vid under vilka betingelser aerosolerna kan aktiveras till CCN. Aerosol-vatten interaktioner påverkar således både de direkta och indirekta klimateffekterna som är associerade med aerosoler, vilket i sin tur påverkar jordens energibudget och i slutändan klimatet. Faktum är, att dessa effekter som aerosolen tros skapa är bland de största osäkerheterna vid bedömningen av vårt framtida klimat. Huvudsyftet med denna avhandling är därför att skapa större kunskap om aerosol-vatten-interaktioner, och därmed bidra till en större förståelse av klimatsystemet som helhet. Avhandlingen har fokuserat på kopplingar mellan aerosolens molekylära sammansättning, dess hygroskopicitet och CCN-aktivering, med fokus på organiska föreningar. Avhandlingen studerar flera vanligt förekommande, förenklade metoder som tillämpas för att beskriva vattenupptag, CCN-aktivering och den resulterande inverkan på aerosolens strålningsegenskaper.

Den traditionella Köhler-teorin som beskriver jämvikten mellan dropp- och ångfasen. Variationer av Köhler-modellen användes tillsammans med olika beskrivningar av interaktionerna mellan vatten och aerosolpartiklar. De modifierade modellbeskrivningarna som användes i denna studie är följande: fullständig upplösning, hygroskopisk parameter ($\kappa$), löslig fraktion ($\varepsilon$), adsorption, samt gas-partikelpartitionering av flyktiga organiska föreningar. Dessutom utvecklade en så kallad ”Solubility Basis Set-modell (SBS)” för att genomföra numeriska studier rörande CCN-aktiveringsbeteendet hos komplexa organiska aerosoler. SBS förlitar sig på en fördelning av lösligheter hos olika kemiska komponenter i dessa blandningar. Utifrån de teoretiska beskrivningarna utvecklades vidare en kopplad hygroskopisk och radiativ transfermodell för att undersöka hur hygroskopisk tillväxt och CCN-aktivering av aerosolpartiklar påverkar aerosolens strålningsegenskaper i Arktiska miljöer och boreala skogsmiljöer. Studierna expanderades även till global skala, och för detta ändamål användes två klimatmodeller (NorESM och ECHAM6-HAM2) med huvudsyfte att studera klimatmodellernas

känslighet beträffande interaktionerna mellan aerosolens organiska ämnen och atmosfärens vatteninnehåll.

Genom tillämpning av ovan beskrivna modelleringsmetoder visades att man utifrån antagandet att en beskrivning som enbart tar hänsyn till SOA-komponenternas begränsad löslighet/löslighetsfördelning inte kan förklara det hygroskopiska beteendet hos SOA i miljöer undermättade med avseende på vattenånga, emedan de kan förklara CCN-aktiveringsbeteendet hos dessa organiska blandningar (dvs. i övermättade miljöer). För att korrekt kvantifiera det hygroskopiska beteendet hos SOA-föreningar i miljöer under 90% relativ fuktighet (RH) krävs inkludering av processer som beskriver adsorptivt vattenupptag, bulk-till-ytseparation, partikelpartitionering av de semivolatila ångorna och icke-idealitet i vätskefaserna med minskande relativ fuktighet ( RH). Å andra sidan beter sig de flesta SOA som nästan helt lösliga i vatten vid övermättnad. Vi fann att skillnaderna i vattenaffinitet hos SOA vid under- och övermättade betingelser kan förklaras av s.k. ”Liquid-Liquid Phase Separation (LLPS)” -effekter. Genom att använda den kombinerade hygroskopicitets- och strålningsöverföringsmodellen kunde en stor effekt på den direkta strålningsbalansen påvisas, beroende på hur vattenupptaget hos aerosolpartiklar beskrivs i Arktisk och boreal skogsmiljö. De globala modellernas bedömning av klimatpåverkan som härrör från OA förlitar för närvarande på grovt förenklade modellbeskrivningar av vattenupptaget hos den annars komplext sammansatta organiska aerosolen. Vi fann att denna enkla, och vanligtvis i klimatmodeller använda parameteriseringen kan introducera betydande fel vid kvantifiering av klimatpåverkan från OA. Resultaten belyser behovet av bättre beskrivningar av växelverkan mellan vattenånga och OA, dess molekylära sammansättning samt global massbalans av OA, med särskild fokus på de för närvarande bristfälligt beskrivna antropogena och marina OA-källorna.

# List of papers and author's contribution

**Paper I: Seasonal variation of aerosol water uptake and its impact on the direct radiative effect at Ny-Ålesund, Svalbard**

N. Rastak, S. Silvergren, P. Zieger, U. Wideqvist, J. Ström, B. Svenningsson, M. Maturilli, M. Tesche, A. M. L. Ekman, P. Tunved and I. Riipinen, Atmos. Chem. Phys., 14, 7445–7460, 2014.

In this study, I developed the coupled hygroscopicity and radiative transfer model and analyzed the experimental data using the model, and wrote most of the paper with contributions from the co-authors.

**Paper II: Connecting the solubility and CCN activation of complex organic aerosols: a theoretical study using solubility distributions**

I. Riipinen, N. Rastak and S. N. Pandis, Atmos. Chem. Phys., 15, 6305-6322, 2015.

In this study, I contributed to the development of the theoretical framework and planning of the model calculations. Furthermore, I conducted most of the model calculations presented in the paper and contributed to writing the paper.

**Paper III: Adsorptive uptake of water by semisolid secondary organic aerosols**

A. Pajunoja, A. T. Lambe, J. Hakala, N. Rastak, M. J. Cummings, J. F. Brogan, L. Hao, M. Paramonov, J. Hong, N. L. Prisle, J. Malila, S. Romakkaniemi, K. E. J. Lehtinen, A. Laaksonen, M. Kulmala, P. Massoli, T. B. Onasch, N. M. Donahue, I. Riipinen, P. Davidovits, D. R. Worsnop, T. Petäjä, A. Virtanen, Geophys. Res. Lett., 42, 3063-3068, 2015.

In this study, I conducted the aerosol radiative effect calculations and contributed to writing the paper and the supplementary information.

**Paper IV: Microphysical explanation of the RH-dependent water-affinity of biogenic organic aerosol and its importance for climate**

N. Rastak, A. Pajunoja, J. C. Acosta Navarro, J. Ma, M. Song, D. G. Partridge, A. Kirkevåg, Y. Leong, W. W. Hu, N. F. Taylor, A. Lambe, K. Cerully, A. Bougiatioti, P. Liu, R. Krejci, T. Petäjä, C. Percival, P. Davidovits, D. R. Worsnop, A. M. L. Ekman, A. Nenes, S. Martin, J. L. Jimenez, D. R. Collins, D. O. Topping, A. K. Bertram, A. Zuend, A. Virtanen, and I. Riipinen, Geophys. Res. Lett., 44, 5167-5177, 2017.

In this study, I conducted most of the thermodynamic model and NorESM calculations and analyzed the results with guidance and help from the co-authors. I wrote the supplementary information and, together with I. Riipinen, the manuscript text, with contributions from the co-authors.

# List of papers not included in the thesis

**Reconciling aerosol light extinction measurements from spaceborne lidar observations and in situ measurements in the Arctic**

M. Tesche, P. Zieger, N. Rastak, R. J. Charlson, P. Glantz, P. Tunved, and H.-C. Hansson, Atmos. Chem. Phys., 14, 7869-7882, 2014.

**Size-resolved cloud condensation nuclei concentration measurements in the Arctic: two case studies from the summer of 2008**

J. Zábori, N. Rastak, Y. J. Yoon, I. Riipinen, and J. Ström, Atmos. Chem. Phys., 15, 13803-13817, 2015.

# Contents

# Abbreviations

| | |
|---|---|
| ADRE | Aerosol Direct Radiative Effect |
| AIOMFAC | Aerosol Inorganic-Organic Mixtures Functional groups Activity Coefficients |
| BF | particle Bounced Fraction |
| CCN | Cloud Condensation Nuclei |
| CCNc | Cloud Condensation Nuclei counter |
| CPC | Condensation Particle Counter |
| c-ToF-AMS | compact Time of Flight Aerosol Mass Spectrometer |
| DMPS | Differential Mobility Particle Sizer |
| FHH | Frenkel-Halsey-Hill |
| HGF | Hygroscopic Growth Factor |
| HR-ToF-AMS | High Resolution Time of Flight Aerosol Mass Spectrometer |
| HTDMA | Hygroscopic Tandem Differential Mobility Analyzer |
| IP | Isoprene |
| IPCC | Intergovernmental Panel on Climate Change |
| MCM | Master Chemical Mechanism |
| MT | Monoterpenes |
| NorESM | Norwegian Earth System Model |
| OA / SOA | Organic Aerosol / Secondary Organic Aerosol |
| PAM | Potential Aerosol Mass flow reactor |
| RH | Relative Humidity |
| SBDART | Santa Barbara Discrete ordinate Atmospheric Radiative Transfer |
| SBS | Solubility Basis Set |
| TOA | Top-Of-Atmosphere |
| VOCs | Volatile Organic Compounds |

# 1. Introduction

In their latest assessment report, the Intergovernmental Panel on Climate Change (IPCC, 2013) put an end to the doubt on whether anthropogenic climate change is occurring or not with a short paragraph: “Warming of the climate system is unequivocal. The atmosphere and oceans have warmed, the amounts of snow and ice have diminished, sea level has risen, and the concentrations of greenhouse gases have increased”. In the same report, the main drivers of climate change are identified as greenhouse gases, atmospheric oxidants, aerosol particles, albedo change due to land use and changes in solar irradiance. As a pronounced example, Arctic temperatures have increased at almost twice the global average rate over the past 100 years, resulting in a steady reduction of Arctic summer sea ice cover and surface albedo since 1979 (Serreze et al., 2007). The Arctic region thus appears to be more sensitive to greenhouse gas-induced warming than the rest of the globe. The Arctic climate is particularly sensitive to changes in northern hemisphere aerosol forcing, which could be induced both by altered particle and precursor emissions as well as atmospheric water content. In general, anthropogenic aerosol forcing has most likely masked a substantial portion of the global mean forcing from well-mixed greenhouse gases (Shindell and Faluvegi, 2009; IPCC, 2013). In fact, aerosols and their climate effects have for a long time contributed to the largest uncertainty when estimating total anthropogenic forcing. Thus, being a key component in the climate system, also improved aerosol representation in models is a key target in reducing the total radiative forcing uncertainty. In this context, a better understanding of the interactions between aerosols and water vapor constitute one of these key targets that is pertinent for our overall understanding of aerosol climate effects.

## 1.1 Atmospheric aerosol particles and their water-vapor interaction in the atmosphere

Atmospheric aerosol particles are solid or liquid particles suspended in air. Aerosol particles can have a wide range of sizes, from a few nanometers (nm) to several tens of micrometers (μm) in diameter (Warneck, 1988). Aerosol particles may enter the atmosphere from natural sources such as oceans, deserts, volcanoes and plants or anthropogenic sources such as open fires, fuel combustion and factories. They can be emitted directly to the atmosphere as particles (primary aerosol) or formed in the atmosphere from gas-to-particle conversion processes (secondary aerosol).

Atmospheric aerosol particles influence the Earth's energy budget directly by scattering and absorbing radiation (Charlson and Pilat, 1969; Coakley et al., 1983) and indirectly by acting as cloud condensation nuclei (CCN) and ice nucleating particles and thereby modifying cloud properties (Twomey, 1977; Albrecht, 1989; Charlson et al., 1992; Ohmann and Feichter, 2005). The estimates of the net aerosol direct and indirect radiative forcing represent the two largest uncertainty terms in the estimate of total anthropogenic forcing (IPCC, 2013).

Chemical analysis of atmospheric aerosol particles shows that most aerosol particles are of a mixed chemical nature, and contain both water-soluble and water-insoluble substances (Junge, 1950). The mix of substances in the water soluble fraction of aerosol particles often cover a wide range of pure-component water solubilities. In the sub-saturated regimes (where RH<100%), atmospheric aerosol particles that contain soluble materials can absorb/evaporate water and grow/shrink in size, which influences their optical properties due to changes in both size and refractive index, resulting in altered scattering and absorption of light, and thus their direct radiative effect (Fitzgerald et al., 1982; Liu et al., 2008; Fierz-Schmidhauser et al., 2010; Zieger et al., 2010, 2013). In the super-saturated regime (where RH>100%), particles of favorable size and composition can efficiently serve as Cloud Condensation Nuclei (CCN) and form cloud droplets if a certain critical supersaturation is reached (referred to as CCN activation), see Fig. 1. Clearly, size and chemistry of aerosol particles largely determine their interaction with ambient water vapor at a given atmospheric relative humidity (RH) as well as their CCN-activation behavior, and therefore the influence that aerosols have on the Earth's radiative forcing and climate.

## 1.2 Complex mixtures of organic aerosol particles in sub- and supersaturated environments

In section 1.1, a more general and somewhat simplified description of aerosol and water vapor interactions was outlined. In the ambient atmosphere, the picture is somewhat more complex. As previously discussed, the contribution of organic material to the global aerosol burden is large. In fact, the organic contribution to the total mass may vary between 20 and 90% depending on location and environment (Kanakidou et al., 2005; Zhang et al., 2007; Jimenez et al., 2009). Of central importance is how interactions between this large organic aerosol fraction and water vapor should be described accurately, both in subsaturated as well as in supersaturated environments. An assessment of this important question is complicated by the fact that aerosol particles are typically found to be complex mixtures of numerous different inorganic and organic components.

While the water uptake of inorganic aerosol particles is considered well-understood (Tang, 1976; Tang et al., 1978, 1997; Ansari and Pandis, 1999), the processes governing the water-interactions of organic aerosol components and their mixtures with the inorganic species are less clear (McMurry and Stolzenburg, 1988; Andrews and Larson, 1993; Saxena et al., 1995; Psfai et al., 1998; Virkkula et al., 1999; Cruz and Pandis, 2000).

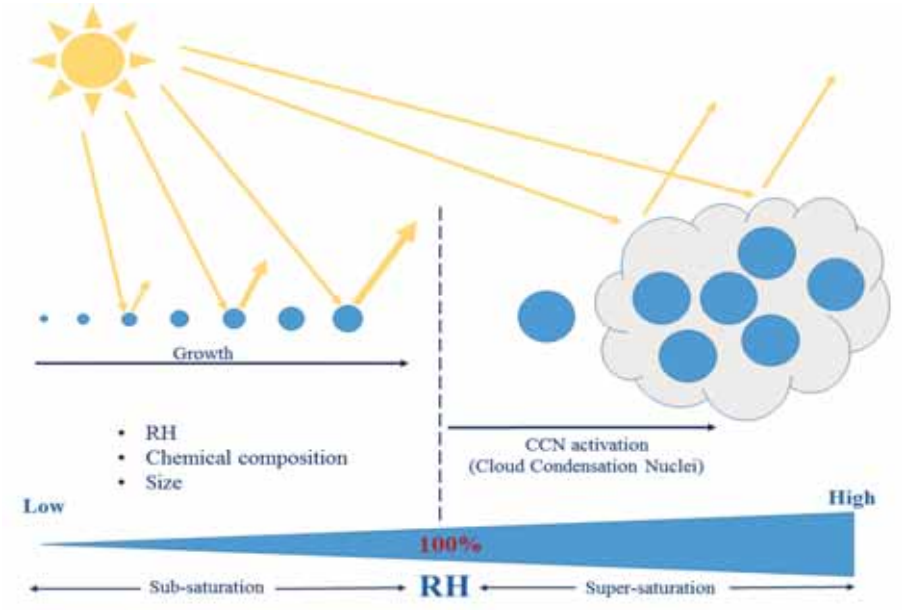


Figure 1: A simple schematic of water uptake by aerosol particles in the ambient atmosphere. At sub-saturation (RH < 100%) aerosol particles grow in size by absorbing water and this hygroscopic growth alters their optical properties. At super-saturation (RH > 100%) they can at some point grow in size serve as CCN to form cloud droplets. Both processes alter the amount of solar radiation that reaches the Earth's surface. The hygroscopic growth and CCN activation behavior of aerosol particles depend on their chemical composition, initial size and ambient RH.

The organic aerosol fraction may consist of thousands of different compounds whose properties, including water solubilities, are poorly known (Golstein and Galbally, 2007; Hallquist et al., 2009; Kroll et al., 2011). This complexity poses a major challenge, hampering the understanding of their atmospheric behavior and resulting climate effects. Forests are one of the main sources of global organic aerosol (OA). Secondary organic aerosol (SOA) are formed through the oxidation of volatile organic compounds (VOCs). Isoprene (IP) and monoterpenes (MT) are the most important precursors of SOA originating from forests. Different types of trees emit

different mixtures of VOCs, resulting in differences in the SOA composition. For instance, the SOA over coniferous forests is dominated by MT oxidation products, while SOA over broad-leaved trees is dominated by IP photooxidation products (Kesselmeier and Staudt, 1999; Guenther et al., 2012). The hygroscopicity and CCN activation behavior of ambient aerosol particles are directly tied to the molecular mechanisms that control aerosol-water interactions. These mechanisms depend highly on the molecular composition of the aerosol and are controlled by parameters such as solubility in water, volatility and oxidation state. While the hygroscopic growth and CCN activation behavior of purely inorganic water-soluble aerosols is relatively straight forward (Asa-Awuku et al., 2007; Topping and McFiggans, 2012; Farmer et al., 2015) and can be explained by Köhler theory (Köhler, 1936), the same processes are not equally well understood for organic aerosols with mixed solubilities. Previous studies have used different approaches to approach the problem and different molecular mechanisms have been used to explain the water affinity of organic aerosols. In some studies, solubility limitations were investigated as the main mechanism that can explain the water affinity of organics (Huff-Hartz et al., 2006), while considered as insoluble compounds in others. For low solubility and insoluble compounds, adsorption has been suggested to be the dominant water uptake mechanism (Sorjamaa and Laaksonen, 2007; Kumar et al., 2009), although bulk to surface partitioning (Ruehl et al., 2016) and gas-particle partitioning of semivolatile gas-phase species (Topping et al., 2011), liquid-liquid phase separation (Song et al., 2012; Krieger et al., 2012; You et al., 2014; Renbaum-Wolff, 2016) or the non-ideality of the mixtures (Kreidenweis et al., 2006; Petters et al., 2009) have been proposed to govern the water upuatke of organic aerosol. It is, however, still unclear which mechanisms control the water affinity of organic mixtures.

### 1.3 Aerosol-water interaction in climate models

Climate models are the tools used for probing the climate system response to changes of some processes or parameters, and this is also the case when trying to determine the climate effect of organic aerosols. However, due to the nature of the interactions between water vapour and complex organic mixtures, the large number of chemical species and intricate molecular interactions, a rigorous treatment of all molecular properties and possible interactions is hindered both by gaps in knowledge as well as by computational limitations. Thus, climate models often rely on crude parameterisations of the interactions between OA and water vapour. Different climate models treat water affinity of organics and its role in quantifying the climate effect of these particles in vastly different manners. For instance, some climate models treat organics as completely water soluble and other as water insoluble when calculating CCN activation. This can lead to more than $\pm 0.4$ $Wm^{-2}$ uncertainty in the aerosol indirect forcing between

preindustrial and present-day conditions (Liu and Wang, 2010). On the other hand, some previous studies have suggested that water-affinity plays only a minor role in determining the climate impact of OA (Betancourt and Nenes, 2014). Due to this ambiguity about atmospheric organics, the organic-water interaction needs to be better understood, thereby reducing the uncertainty caused by organics in climate predictions.

### 1.4 Objectives

The main goal of this thesis was to investigate the interaction between water vapor and atmospheric aerosol particles in both sub-saturated and super-saturated conditions. The main objectives and related questions were:

**Objective A: To investigate the links between aerosol molecular composition, hygroscopic growth and CCN activation, with a focus on organic compounds.**

(1) Which microphysical mechanisms govern the aerosol-water interactions (Papers I, II, III and IV)?

(2) Why has a discrepancy between the sub-and supersaturated conditions for organic aerosol water uptake been observed in experimental data (Papers III and IV)?

**Objective B: To test simplifying approaches for describing water uptake, CCN activation and their impact on radiative properties.**

(1) Can the hygroscopic growth and its effect on the radiative properties of Arctic aerosol be predicted from observations of size distribution and chemical composition (Paper I)?

(2) How many parameters are needed to describe the solubility of organic aerosol in CCN activation (Paper II)?

(3) How large error do we introduce because of the highly simplified schemes of organic aerosol used in climate models (Papers III, IV)?

I will first discuss the various theoretical approaches we used to describe the interactions between aerosol particles and water vapor. I will then outline the different sources of data and model tools we used in our work. I will then present highlights from the papers included in the thesis to illustrate how we met the objectives of our research.

# 2. Theoretical background

In the atmosphere, water may be encountered in gas, liquid or solid phases. In the aqueous phase, water may appear as either water droplets or in the form of wetted aerosol particles. In its simplest form, over a flat surface of pure water, partial pressure of the gaseous phase over the liquid surface will be equal to the saturation vapor pressure of pure water at the given temperature. Soluble material in the aqueous phase tends to lower the equilibrium water vapour pressure over the surface, thus shifting the equilibrium towards the aqueous phase. At the same time, considering the size scale of water droplets, also the curvature of the droplet comes into play. This is an effect largely determined by the surface tension of water, and it results in an increase in the equilibrium water vapour pressure over the droplet as the size gets smaller. These two effects, Raoult and Kelvin effect respectively, together thus either increase or decrease the water equilibrium vapour pressure over atmospheric aqueous droplets. The Raoult effect becomes larger with increasing concentration of solutes, and the Kelvin effect decreases with size. Their combined effect on water equilibrium in the atmosphere can be described by Köhler theory. In very simple words, a large, soluble particle has a greater affinity for water as compared to a small, insoluble particle.

This chapter will provide a more detailed background on Köhler theory and explore the different assumptions and parameterisations applied in studies of hygroscopic growth and CCN activation in the atmosphere. The parts of sections 2.1 and 2.2 in quotation marks build directly upon the theories presented in my licentiate thesis (Rastak 2014) and the supplementary information of Paper IV (Rastak et al., 2017).

## 2.1 Equilibrium between droplet and vapor phase (Köhler theory)

"When an aerosol particle absorbs water and grows in size, the equilibrium size of the formed droplet, its chemical composition and water content can be linked to the ambient water vapor saturation ratio *S* through the traditional Köhler equation (Köhler, 1936).

$$S = \frac{p_{w,eq}}{p_{w,sat}} = a_w \exp\left(\frac{4\sigma M_w}{RT\rho_w D_{p,wet}}\right), \quad (1)$$

where $p_{w,eq}$ (Pa) is the equilibrium vapor pressure of water over the droplet surface, $p_{w,sat}$ (Pa) the saturation vapor pressure over a pure flat water

surface, $\sigma$ (N m$^{-1}$) is the surface tension of droplet, $M_w$ (kg mol$^{-1}$) the molar mass of water, $\rho_w$ (kg m$^{-3}$) the density of water, $D_{p,wet}$ (m) the diameter of the droplet, $T$ (K) the temperature and $R$ (J mol$^{-1}$ K$^{-1}$) the universal gas constant. The water activity ($a_w$) is defined as the product of the water mole fraction $X_w$ and water activity coefficient in the aqueous phase $\Gamma_w$,

$$a_w = X_w \Gamma_w . \quad (2)$$

The activity coefficient describes the interactions between water molecules and the dissolved molecules in the mixture. Assuming ideal interactions between water and dissolved molecules results in $\Gamma_w$=1. As $a_w$ explains the role of dissolved material in the aqueous phase and is defined by Raoult's law, it is known as Raoult (or solute) effect. The exponential part in Eq. 1 is defined by the droplet size and it is known as Kelvin (or curvature) effect.Note that instead of saturation ratio ($S$), often supersaturation ($s$), defined as $s = S - 1$, is used. An example of the $S$ ($D_{p,wet}$) curve, known as the Köhler curve is shown in Fig. 2. The exact shape of the Köhler curve depends on the size and composition of the dry aerosol particle (and thus the resulting droplet). The maximum in the Köhler curve is known as the critical point and plays an important role in determining the behavior of the droplet in ambient atmosphere. The droplet diameter and supersaturation at this point are called the critical droplet diameter ($D_{p,\ wet,c}$) and critical supersaturation ($s_c$), respectively. As we move along the Köhler curve on the ascending branch, the droplet is in stable equilibrium with its environment. Assuming a fixed saturation ratio, this means that if the droplet grows slightly in size with the addition of a few water molecules, its equilibrium vapor pressure is higher than the ambient at this new larger size, and the droplet will evaporate water and return to its original size. If a few water molecules are subtracted from the droplet, its saturation vapor pressure will become lower than the fixed ambient value and water will condense on the droplet returning it to its original size. On the other hand, on the descending branch of the curve, if droplet grows in size by addition of a few water molecules, its equilibrium vapor pressure becomes lower than the fixed ambient value and water will condense on the droplet and it will grow even larger. If the droplet loses a few water molecules as its equilibrium vapor pressure becomes higher than the ambient, the water evaporates from the droplet and it will shrink even more. Therefore the droplet on the descending branch of the Köhler curve is in unstable equilibrium with its environment (Seinfeld and Pandis, 1998).

If the ambient $S$ or RH is not fixed, by moving along the ascending branch of the Köhler curve in the sub-saturated regime ($S < 1$ or RH < 100%) as $S$ or RH increases, the particle remains solid until RH reaches a value where the solid particle spontaneously absorbs water, producing a saturated aqueous solution. Increasing the ambient RH leads to additional water condensation onto the aqueous solution and makes the particle to grow in size. If $S$ or RH

increases in the super-saturated regime ($S > 1$ or RH > 100%), while ($1 < S < S_c$) the droplet will continue growing. If the ambient saturation ratio $S$ exceeds the particle critical saturation ratio $S_c$ then the particle will grow without bounds even if the ambient S decreases, eventually forming a cloud droplet. This process is called CCN activation. The critical point is also known as the activation point (Seinfeld and Pandis., 1998)."

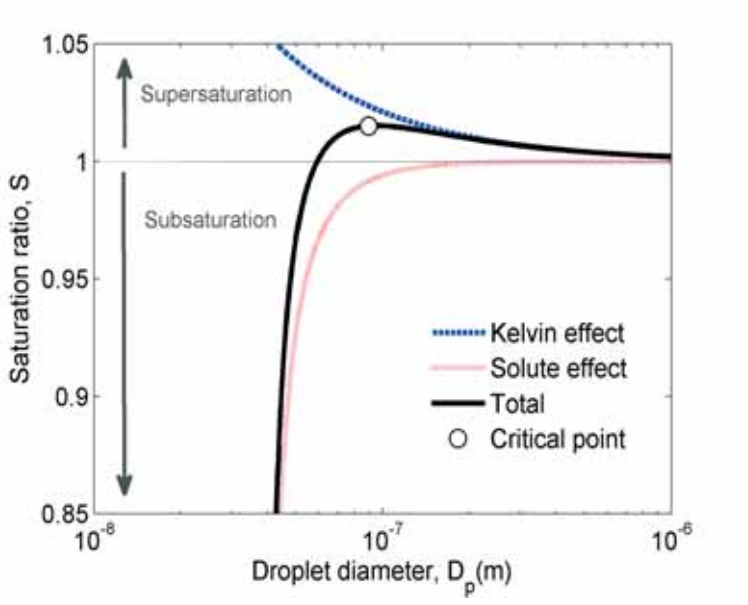


Figure 2: An example of a Köhler curve illustrating the competition between the curvature (Kelvin) and solute (Raoult) effects. While ambient saturation ratio is lower than the saturation ratio at the critical point as ambient saturation ratio increases, the particle grows in size by absorbing water. When the ambient saturation ratio exceeds the saturation ratio at the critical point the particle is activated and grows in size with no limitation and can serve as a cloud condensation nucleus (CCN).

## 2.2 Parameterisations describing hygroscopic growth and solubility

The original Köhler theory predicts hygroscopic growth and CCN activity based on the aerosol physicochemical properties, i.e. solute mass, molecular weight, bulk density, dissociable ions, and activity coefficient (Petters and Kreidenweis, 2007). Therefore, it requires detailed knowledge of each compound. This theory can explain the hygroscopic growth and activity of pure soluble particles, but it needs some modifications for less- and non-hygroscopic organics and also organic-inorganic mixtures. Here we present some of these simplifications and modifications built on the original Köhler theory.

### 2.2.1 Complete dissolution assumption

"This assumption simplifies the aerosol water uptake and CCN activation by assuming that all the material in the mixed particles is fully soluble and can be completely dissolved at all conditions where water is present (Raymond and Pandis, 2002). This simplification has shown to work in interpreting some laboratory measurements of CCN activation of organic single- and multi-component aerosol particles (e.g. Huff Hartz et al., 2006; Chan et al., 2008). The laboratory studies by Chan et al. (2008) indicate that the CCN activation of material with water solubility as low as 1 g $L^{-1}$ could be predicted assuming complete dissolution. Huff Hartz et al. (2006) suggested that compounds with water-solubilities above 3 g $L^{-1}$ behaved as if they were completely soluble in water."

### 2.2.2 Hygroscopicity parameter (κ) and soluble fraction (ε)

"In many practical applications the water activity ($a_w$) and the difference in the densities and molar masses of water and the dry material are expressed with a single hygroscopicity parameter ($\kappa$), introduced by Petters and Kreidenweis (2007), defined as

$$\frac{1}{a_w} = 1 + \kappa \frac{V_s}{V_w} \cdot \tag{3}$$

Where $V_s$ and $V_w$ are the volumes of the dry material and water, respectively. Assuming additive volumes, the traditional Köhler equation can be reformulated to the $\kappa$-Köhler equation,

$$S = \frac{D_{p,wet}^3 - D_{p,dry}^3}{D_{p,wet}^3 - D_{p,dry}^3(1-\kappa)} \exp\left(\frac{4\sigma M_w}{RT\rho_w D_{p,wet}}\right) \tag{4}$$

Where $D_{p,dry}$ (m) is the initial dry diameter. In some studies you can find this equation as a function of hygroscopic growth factor *HGF*, defined as

$$HGF = \frac{D_{p,wet}}{D_{p,dry}} \cdot \tag{5}$$

For a multicomponent system, the overall value for $\kappa$ is given by a simple mixing rule,

$$\kappa = \sum_i \alpha_i \kappa_i \tag{6}$$

Where $\alpha_i$ defines the dry volume fraction of each component as $\alpha_i = \frac{V_{si}}{V_s}$ and $\kappa_i$ is the hygroscopicity parameter for compound *i*.

Equation 4 results in an approximate expression for the relationship between $s_c$ (critical supersaturation) and $D_{p,act}$ (activation diameter) defined as

$$s_c = \frac{2}{3}\left(\frac{4M_w\sigma}{RT\rho}\right)^{3/2}\left(3\kappa D_{p,act}^3\right)^{-1/2} \quad (7)$$

For an ideal solution of water and a solute, the $\kappa$ is directly proportional to the dissolved fraction and the ratio of the molar volumes of water and the solute i.e. $\kappa = \varepsilon\kappa_{max}$, where $\kappa_{max} = M_w/M_s \cdot \rho_s/\rho_w$ (Asa-Awuku et al., 2010), $M_w$ and $M_s$ are the water and solute molar mass, and $\rho_w$ and $\rho_s$ the water and solute density, respectively. Assuming that a single soluble fraction $\varepsilon$ can represent a given mixture at all considered supersaturations, and introducing these relationships into Eq. 7 yields"

$$s_c = \frac{2}{3}\left(\frac{4M_w\sigma}{RT\rho}\right)^{3/2}\left(3\frac{M_w}{M_s}\frac{\rho_s}{\rho_w}\varepsilon D_{p,act}^3\right)^{-1/2} \quad (8)$$

### 2.2.3 Frenkel, Halsey and Hill (FHH) adsorption theory and its combination with Raoult and Kelvin effects

"While Eq. 1 describes well the hygroscopic growth and cloud droplet activation of aerosol particles dominated by highly water-soluble compounds, it does not describe the surface interactions through adsorption of water molecules onto insoluble surfaces – although these might become important for the water-uptake of predominantly insoluble particles. For instance, Raymond and Pandis (2002) discovered that organic species with low solubility in water can act as CCN in the atmosphere if they are wettable by water (i.e. their contact angle with water is 0). One possible alternative for explaining the CCN activation behavior of such wettable organic species with low solubility in water is multilayer adsorption theory. The adsorption theory by Frenkel, Halsey and Hill (FHH) is one of the most well-known adsorption models and has been widely used (Frenkel, 1946; Halsey, 1948, 1964; McDonald, 1964; Jiusto and Kockmond, 1968; Hill, 1949; Sorjamaa and Laaksonen, 2007; Kumar et al., 2009, 2011a-b). If the surface of the insoluble particle is wettable, the attractive forces between the water molecules and the surface help to form uniform layers of adsorbed water molecules over the particle surface. For particles with negligible solubility, the water activity ($a_w$) in Eq. 1 can be substituted with the FHH isotherm (Kumar et al., 2011a),

$$a_w = \exp(-A_{FHH}\theta^{-B_{FHH}}). \quad (9)$$

The FHH isotherm is defined by three parameters, namely surface coverage $\theta$ (the number of adsorbed water molecules divided by the number of molecules in a monolayer) and two empirical constants ($A_{FHH}$ and $B_{FHH}$), known as adsorption coefficients. $A_{FHH}$ characterizes interactions of adsorbed molecules with the insoluble aerosol particle surface and adjacent adsorbate molecules (i.e., those in the first monolayer). $B_{FHH}$ characterizes the

attraction between the insoluble particle surface and the adsorbate in subsequent layers; the smaller the value of $B_{FHH}$, the greater the distance over which the attractive forces act.

Combining Eqs. 1 and 9, the equilibrium saturation ratio for a solution droplet containing an insoluble wettable core is obtained from"

$$S = \exp(-A_{FHH}\theta^{-B_{FHH}}) \exp\left(\frac{4\sigma M_w}{RT\rho_w D_{p,wet}}\right). \quad (10)$$

The adsorption theory on its own assumes that aerosol particles are insoluble but wettable and can take up water only via surface adsorption. In the case of aerosol particles containing a soluble fraction, however, we need a theory that takes into account the possibility of this soluble fraction being dissolved in the adsorption layer (Kumar et al., 2009). Assuming that the adsorbed water on the surface of the insoluble core is in equilibrium with the aqueous phase and water vapor, the water activity that accounts for both the Raoult (solute) and adsorption effects is defined as

$$a_w = X_w \Gamma_w \exp(-A_{FHH}\theta^{-B_{FHH}}). \quad (11)$$

Therefore, the equilibrium saturation ratio for a solution droplet containing a wettable core surrounded by an aqueous phase (i.e. a mixture of water and the soluble fraction) is obtained from"

$$S = X_w \Gamma_w \exp(-A_{FHH}\theta^{-B_{FHH}}) \exp\left(\frac{4\sigma M_w}{RT\rho_w D_{p,wet}}\right). \quad (12)$$

### 2.2.4 Effective particle hygroscopicity when accounting for semi-volatile compound partitioning

"It is worth noting that the particle diameter at humidified conditions can be different from $D_{p,dry}$ for two reasons: (1) water uptake according to the hygroscopicity of the particle's "solute" mixture and (2) a change in actual water-free particle mixture composition may occur due to gas-particle partitioning of semivolatile components (which could be a net loss or gain of particulate material). The classical Köhler theory (Eq. 1) and Eq. 4 of the κ-Köhler theory both ignore the second, partitioning-related point and implicitly assume that all solute material is non-volatile. Accounting for the potential change in solute mixture composition as RH changes, affecting $D_{p,wet}$ and HGF, a more general definition of the effective hygroscopicity parameter κ is derived starting from Eq. 3:

$$\frac{1}{a_w} = 1 + \kappa \frac{V_{s,0}}{\left(V_w + V_s - V_{s,0}\right)}. \quad (13)$$

Here $V_{s,0}$ represents the dry mixture (solute) volume at a reference RH level, typically chosen to be at RH = 0 % (i.e. water-free), while $V_s$ represents the water-free particulate matter volume at the present RH level. Thus, $V_s + V_w = V_p$, with $V_p$ the overall particle volume. Note that Eq. 13 reduces to Eq. 3 when the solute mixture is non-volatile such that $V_s = V_{s,0}$ at all particle sizes and RH levels.

Consistent with Eqs. 4 and 13, the effective particle hygroscopicity is calculated by the following expression:

$$\kappa_{HGF} = 1 - HGF^3 + \frac{HGF^3 - 1}{S} \exp\left( \frac{4\sigma M_w}{RT\rho_w D_{p,wet}} \right). \quad (14)$$

Equation 14 can be simplified by substituting Eq. 1 for S, which leads to cancellation of the Kelvin effect factor exp […],

$$\kappa_{HGF} = 1 - HGF^3 + \frac{HGF^3 - 1}{a_w} = (HGF^3 - 1)\left( \frac{1}{a_w} - 1 \right) \quad (15)$$

This is meaningful when the actual water activity is known, e.g., in the case of thermodynamic model calculations in which water activity is determined solely by the particle composition (and therefore linked to HGF)."

# 3. Materials and Methods

This section contains a brief description of the data sets and models we used to investigate the interaction of water vapor with atmospheric aerosol particles in the papers constituting this thesis. In the first section (Sect. 3.1), the thermodynamic modeling approaches that we used throughout the thesis are explained. In the following sections (Sect. 3.2 and 3.3), the data and models used to address objectives A and B are summarized.

## 3.1 Aerosol-water interaction and thermodynamic modeling approaches

The way that aerosol particles interact with water depends on their chemical composition and related parameters such as solubility, volatility, oxidation state. These interactions can be described assuming a range of simplified or more comprehensive theoretical descriptions considering detailed molecular processes and mechanisms. A schematic representation of four possible thermodynamic modeling approaches is shown in Fig. 3. Note that there are more possible approaches to explain aerosol-water interaction, but only the approaches which were used in this study are mentioned here.

**Complete dissolution:** One of the simplest approaches is to assume complete dissolution. In this assumption, aerosol particles consist of high-soluble compounds, which can be dissolved in water over the entire RH range starting from low RH values. In this assumption, we only have one aqueous phase which is in equilibrium with ambient water vapor. This approach was used in Paper II, see Sect. 2.2.1.

**Simple dissolution:** In this approach, we assume that aerosol particles are mixtures of different nonvolatile compounds with a range of solubilities from low to high values. We have an insoluble core surrounded by the aqueous phase. The insoluble core is in equilibrium with the aqueous phase and the aqueous phase is in equilibrium with the ambient water vapor. In this approach traditional Köhler, κ-Köhler, soluble fraction (ε) from the theory section were used, see Sect. 2.2.2. This approach was used in Papers I and II.

**Simple dissolution + adsorption:** Here, we have the same assumptions as simple dissolution plus the adsorption of water molecules on the insoluble core. In this approach the FHH adsorption theory was used, see Sect. 2.2.3. This approach was used in Paper III.

**Liquid-liquid phase separation (LLPS) + gas-particle partitioning**: In the last and most comprehensive approach, we assumed semi-volatile and

volatile compounds. Therefore, we have gas-particle partitioning of the organic vapors and water. We have liquid-liquid phase separation (LLPS), therefore there are two phases, a water-rich phase and an organic-rich phase, of which the latter is at the surface and the former is in the centre. These two phases are in equilibrium with each other and the ambient water vapor. We also have surface tension reduction by organics on the outer layer of the insoluble coating. In this approach the hygroscopic growth theory accounting for semivolatile compound partitioning was used, see Sect. 2.2.4. All these four approaches were used in Paper IV.

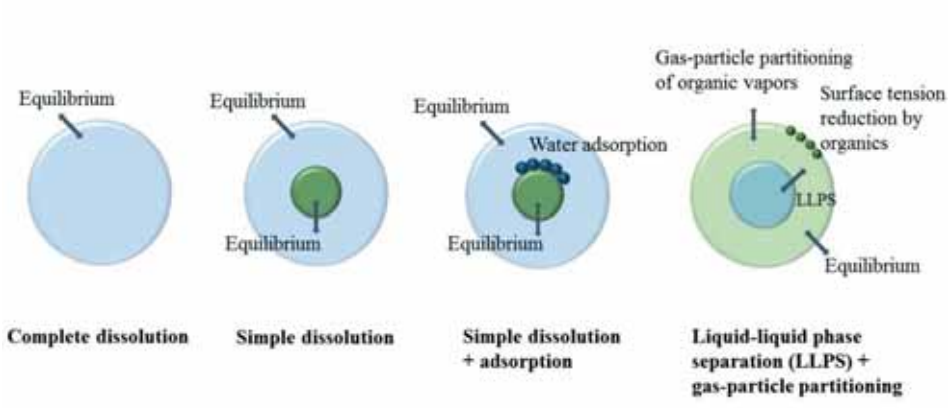


Figure 3: A schematic representation of four possible thermodynamic modeling approaches to explain the aerosol-water interaction. Starts from simple complete dissolution to more comprehensive ones considering adsorption, LLPS and gas-particle partitioning.

### 3.2 Data and models used to approach Objective A: *To investigate the links between aerosol molecular composition, hygroscopic growth and CCN activation, with a focus on organic compounds*

Our approach was to constrain theoretical results to match the experimental and field data sets for particles formed from different organic precursors. We used two of different thermodynamic modeling approaches. In the first approach (simple dissolution + adsorption), the solubility distributions of IP and MT SOA were used in the Solubility Basis Set (SBS) model coupled with a treatment of adsorption using the FHH adsorption theory (Sect. 2.2.3). To explore the non-ideal behavior further, we used the multiphase system online property prediction (UManSysProp, see section 3.2.2.3) for calculating $\Gamma_w$ in organic solution droplets. For calculating activity coefficients in aqueous solutions the Aerosol Inorganic-Organic Mixtures Functional groups Activity Coefficients (AIOMFAC, see section 3.2.2.2) model was applied within UManSysProp. In the second approach (LLPS + gas-particle partitioning), a gas-particle partitioning model based on AIOMFAC and the pure compound liquid-state saturation vapor pressure

prediction model EVAPORATION was used, see Sect. 3.2.2.2. This equilibrium gas-particle partitioning model includes the prediction of a potential liquid-liquid phase separation (LLPS) in the liquid particle mixture. To visually observe the phase state behavior of the two SOA types, optical images of micrometer scale SOA particles were used, see Sect. 3.2.1.1.

### 3.2.1 Data used

Below we give a brief presentation of the data used to approach research Objective A. Both data from laboratory experiments and data from field measurements were used. The parts of chapter 3 in quotation marks build directly upon the text presented in the supplementary information of Paper III and IV.

#### 3.2.1.1 Laboratory data

"We used the laboratory data set for particles formed from isoprene ($C_5H_8$), α-pinene ($C_{10}H_{16}$), and longifolene ($C_{15}H_{24}$) precursors. Pure SOA particles were formed in a continuous flow Potential Aerosol Mass flow reactor (PAM) (Kang et al., 2007; Liu et al., 2015). SOA precursors react with $O_3$ or OH radicals inside the reactor, after which low-vapor pressure oxidation products homogenously nucleated to form SOA particles. Then (a) sub-saturated water uptake (hygroscopic growth, HGF) using HTDMA, (b) supersaturated cloud-droplet formation using a Cloud Condensation Nuclei counter (CCNc , Roberts and Nenes, 2005; Lance et al., 2006), (c) particle bounced fraction (BF) using an Aerosol Bounce Instrument, and (d) SOA oxidation state using a compact time of flight aerosol mass spectrometer (c-ToF-AMS) were measured.

Optical images of SOA derived from ozonolysis of α-pinene have been reported previously (Renbaum-Wolff et al., 2016), and this section is concerned with optical imaging of SOA formed from photo-chemical oxidation of isoprene. Isoprene-derived SOA was generated by the photo-oxidation of isoprene in an oxidation flow reactor (Kang et al., 2007; Lambe et al., 2011; Liu et al., 2015). Particles formed in the reactor were collected on a hydrophobic glass slide at the exit of the flow reactor set-up using a single stage impactor or electrostatic precipitator (Renbaum-Wolff et al., 2016). After collection, the hydrophobic glass slide was inserted into a temperature and relative humidity controlled flow cell coupled to an optical microscope (Zess Axiotech, 50 × objective). RH was controlled within the cell by varying the ratio of a dry and humidified $N_2$ flow with the total flow rate of ~1200 sccm. The RH was measured using a hygrometer with a chilled mirror sensor (General Eastern, Canada), which was calibrated using deliquescence RH for pure ammonium sulfate particles (uncertainty of the RH: ±1.0 %). After the glass slide containing the SOA particles was inserted

into the flow cell, the SOA particles were equilibrated at ~100 % RH for 15 min, and then the RH was scanned over a decreasing RH interval of ~100 to ~0 % and subsequently over an increasing RH interval ranging from ~0 to ~100 % RH at a RH change-rate of 0.1 - 0.5 % RH $min^{-1}$. During the humidity cycles, optical images of the SOA particles were recorded every 5 - 10 seconds using a CCD camera. All experiments were performed at constant temperature of 290 ± 1 K. From the optical images, the presence of one or multiple phases could be identified."

#### 3.2.1.2 Field data

"Ambient measurements comprised comprehensive measurement campaigns carried out in the Southeastern US, Centreville, Alabama (32.90289°N, 87.24968°W, 126 m asl.) (Hu et al., 2015; Xu et al., 2015), and in Northern Europe, Finland, Hyytiälä (61.84524°N, 24.28883°E, 181 m asl.) in the summer of 2013. Both sites are rural environments with dominance of biogenic emission sources. The chemical composition in Alabama and Hyytiälä is dominated by IP (Kaiser et al., 2016) and MT (Hakola et al., 2003; Raatikainen et al., 2010; Finessi et al., 2012), respectively. The airborne particle population was characterized by size and composition with a Differential Mobility Particle Sizer (DMPS) and HR-ToF-AMS, respectively. Moreover, the hygroscopic properties of the particles were measured both at sub- and supersaturated conditions with HTDMA and CCNc instruments, respectively. Humidity control in the HTDMA and CCNc were similar to the laboratory measurements, but the water saturations in the setups were fixed to RH = 90% and SS = 0.2%, respectively."

### 3.2.2 Modelling tools used

Below follows a description of the various modelling tools needed to answer the research objective A.

#### 3.2.2.1 Solubility Basis Set (SBS) and Solubility distributions of IP- and MT-SOA

In order to account for the large range of different solubilities present in organic aerosols we applied the method of the solubility basis set (SBS). We considered a monodisperse population of spherical aerosol particles consisting of an internal mixture of organic compounds. When exposed to water vapor, these particles were assumed to grow reaching a thermodynamic equilibrium between the water vapor and the particle phase. The wet particle was allowed to consist of maximum two phases: the insoluble organic phase and the aqueous phase. The composition of the organic and aqueous phases was determined on one hand by the equilibrium

between the aqueous phase and water vapor, and on the other hand by the equilibrium of the aqueous phase with the organic insoluble phase (Fig. 4).

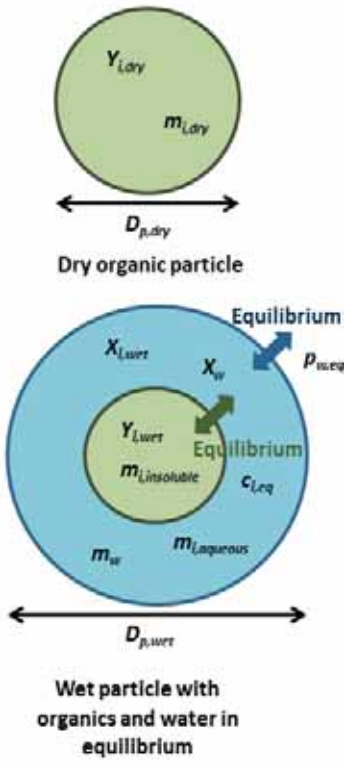


Figure 4: The conceptual model of the equilibrium composition calculations. The dry particle is assumed to consist of n organic compounds, each denoted with a subscript i. The wet particle is assumed to consist of a dry organic (insoluble) phase and an aqueous phase with water and dissolved organics. The aqueous phase is assumed to be in equilibrium with the ambient water vapor. Y refers to mole fractions in the dry organic phase, X to mole fractions in the aqueous phase, and m to the masses of the organic constituents and water. $c_{i,eq}$ refers to the equilibrium concentration of each organic compound in the aqueous solution and $p_{w,eq}$ to the equilibrium vapor pressure of water above the aqueous solution.

The mixture was represented by n surrogate compounds with varying solubilities. By varying the range of pure component water solubilities present in the mixture, the shape of the solubility distribution, and the number of components n in the distribution, we ended up with 72 different organic mixtures of different solubility distributions. In addition, by assuming two different kinds of interactions between the organic compounds in the insoluble phase we ended up with 144 organic mixtures. The assumptions used where: 1) ideal mixture, where organics limit each other's dissolution and; 2) unity activity, where organics behave as pure compounds

and do not influence each other's dissolution. Critical supersaturations and the dissolution behavior at the point of CCN activation were calculated utilizing the Köhler theory for all organic mixtures.

The SOA surrogate molecules, predicted by the Master Chemical Mechanism (MCM; http://mcm.leeds.ac.uk/MCM, Chen et al., 2011), were used for predicting solubility distributions of isoprene and monoterpene SOA by the SPARC model (Hilal et al., 1995). These solubility distributions were used in Papers II and IV. In our calculations, the mole-weighted average molar masses of 150 g $mol^{-1}$ and 195 g $mol^{-1}$ and the average mass densities of 1480 kg $m^{-3}$ and 1230 kg $m^{-3}$ were used for IP and MT, respectively. A list of MCM species can be found in Table S2 and S3 (supplementary information Paper IV), see also Fig. 5.

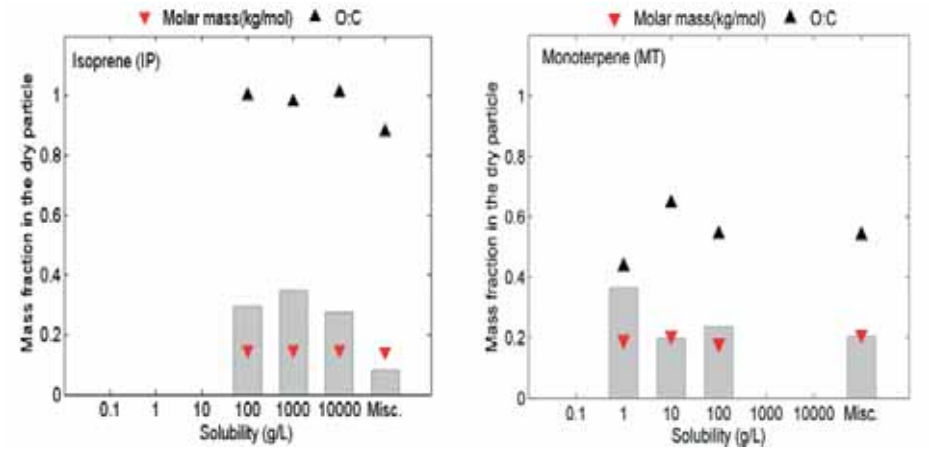


Figure 5: A) The solubility distribution assumed for isoprene (IP). IP with a high oxygen-to-carbon ratio (O:C = 1.07) has high water solubility, ranging from 100 g $L^{-1}$ to fully soluble. B) The solubility distribution assumed for monoterpene (MT). MT with (O:C = 0.54) is less soluble in water than IP with values mainly between 0.1 and 100 $gL^{-1}$ and about 20% of mass in the Misc (miscible) bin. The solubility value for Misc bin was $10^5$ $gL^{-1}$.

### 3.2.2.2 AIOMFAC-EVAPORATION model

The AIOMFAC-based framework is a thermodynamic equilibrium model for gas-particle partitioning (Compernolle et al., 2011; Zuend and Seinfeld, 2012). The gas-particle partitioning was operated on the assumption that the SOA mixtures are in a liquid (potentially viscous) state and may therefore absorb (rather than adsorb) an amount of water depending on the level of RH. In addition, the model includes the algorithm developed by Zuend and Seinfeld (2013) for the prediction of a potential liquid-liquid phase separation as a function of overall liquid mixture composition. The pure

component liquid state saturation vapor pressures for SOA components were computed for a temperature of 298.15 K using the EVAPORATION model (Compernolle et al., 2011), available online at http://tropo.aeronomie.be/models/evaporation_run.htm.

#### 3.2.2.3 UManSysProp

The multiphase system online property prediction (UManSysProp) is an online application developed for calculating the properties of individual molecules, mixtures (organic, inorganic or mixed organic-inorganic) and aerosol particles, available online at http://vm-woody009.itservices.manchester.ac.uk/index.

### 3.3 Data and models used to approach Objective B: *To test simplifying approaches for describing water uptake, CCN activation and their impact on radiative properties*

We developed a coupled hygroscopicity and radiative transfer model to examine if the hygroscopic growth and its effect on the radiative properties of Arctic aerosol can be predicted from observations of size distribution and chemical composition. Besides, with the coupled model we were able to look into the seasonality of hygroscopicity, optical properties and radiative impact of aerosol particles. We further explored the sensitivity of aerosol-climate interactions to the description of OA water-uptake and CCN activation in global models, and the role of solubility in CCN activation of organic aerosols was investigated using the SBS model.

### 3.3.1 Theoretical investigation of simplifying assumptions on solubility

In Paper II, the SBS model predictions of hygroscopic growth and CCN activation behavior of organic mixtures were compared with the three simplified models: 1) assuming complete dissolution of all compounds 2) treating the organic mixture solubility with the hygrosopicity parameter κ and 3) assuming a fixed soluble fraction ε for each mixture. The SBS model is described in detail in Sect. 3.2.2.1.

.

### 3.3.2 Coupled hygroscopicity and radiative transfer model

To examine the effect of hygroscopic growth on aerosol optical properties and the aerosol direct effect, three different models were coupled together. Therefore, we call this model ‘coupled hygroscopicity and radiative transfer model’. First, we modelled the hygroscopic growth of aerosol particles in ambient atmosphere using the κ-Köhler theory (Petters and Kreidenweis,

2007, Sect. 2.2.2). In the next step, we investigated the effect of this hygroscopic growth on aerosol optical properties by coupling the hygroscopic model to a Mie scattering model (Wiscombe, 1979). Finally, a radiative transfer model (SBDART, Ricchiazzi et al., 1998) was used to look into the local effect of hygroscopicity on Aerosol Direct Radiative Effect (ADRE).

We applied the coupled hygroscopicity and radiative transfer model for the Artic environment in Paper I and for the boreal forest environment in Paper III. In Paper I, observational data including number size distribution, chemical composition and RH collected at the Zeppelin research station in Ny-Ålesund, Svalbard for year 2008 were used. In Mie theory, the ability of aerosol particles to scatter or absorb radiation was described through their scattering coefficient ($\sigma_{sp}$) and absorption coefficient ($\sigma_{ap}$). The total radiant energy that can be scattered or absorbed by aerosols was defined by their extinction coefficient ($\sigma_{ext} = \sigma_{sp} + \sigma_{ap}$). The calculated ADRE with the radiative transfer model was defined as the difference in surface net flux due to aerosol loading. In the calculations we assumed an internal mixing state and a homogeneous chemical composition for the whole particle size range (10-790 nm). Aerosol chemical composition was determined from filter measurements. Chemical speciation was made using two different observational data sets: one for the division between organic and elemental carbon (OC/EC) and inorganic aerosol components, and one for attaining the composition of the inorganic aerosol fraction. In Paper III, this model was used to calculate ADRE and the relative change in ADRE using the hygroscopic kappa $\kappa_{HGF,}$ and CCN kappa $\kappa_{CCN}$. These kappa values were calculated using the mixing rule (Eq. 6) and the mass fractions measured at Hyytiälä station in Finland. The calculations were conducted by using three different RH profiles (25, 50 and 75 percentile), see Fig. S8 in the supplementary information of Paper III. A scheme of the models and their required inputs is shown in Fig. 6.

#### 3.3.2.1 Mie model

The interaction of a single spherical particle with radiation can be computed from Mie theory (van de Hulst, 1957; Kerker, 1969; McCartney, 1976). The Mie model, MIEV0 by Wiscombe (1979) was used in Papers I and III. The entire package of numerical code is available from the internet server http://www.scattport.org/index.php/light-scattering-software?start=100. The Mie model was run, assuming aerosol particles as homogenously mixed spheres.

#### 3.3.2.2 Radiative transfer model (SBDART)

We used the Santa Barbara DISORT (discrete ordinate) Atmospheric Radiative Transfer model (SBDART) for calculating the solar irradiance for clear sky conditions (Ricchiazzi et al., 1998). The investigated wavelength range covers 0.25 to 4 µm using a wavelength increment of 0.005 µm. The radiative transfer model requires the atmospheric profiles of pressure (hPa), temperature ($K$), water vapor density ($gm^{-3}$) and ozone density ($gm^{-3}$). The required model input of the aerosol optical depth (AOD), single scattering albedo $\omega$, and the asymmetry parameter $g$ of the phase function at each atmospheric layer were calculated using the Mie model over the indicated wavelength range using observations of aerosol number size distribution and chemical speciation, with hygroscopic growth taken into account, as previously described. The solar zenith angle was predefined in the code according to the time of the day, time of year and geographical coordinates.

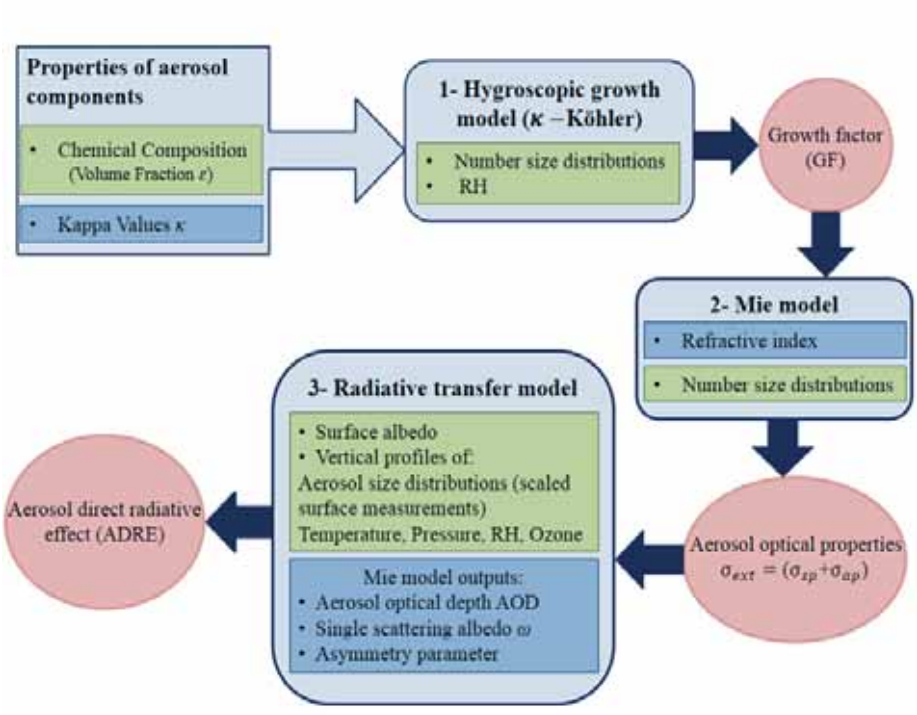


Figure 6: Scheme of the coupled hygroscopicity and radiative transfer model and the required input, starting with the hygroscopic growth model and ending with the radiative transfer model to calculate the aerosol direct radiative effect (ADRE). The light blue boxes refer to the different model calculations, the green boxes to experimental input data, and the dark blue boxes to additional input data (e.g. from literature), and the red circles denote model output.

### 3.3.3 Sensitivity of aerosol-climate interactions to the description of OA water-uptake

We explored the sensitivity of aerosol-climate interactions to the description of OA water-uptake and CCN activation by setting up simulations with two global models, NorESM and ECHAM6-HAM2.

#### 3.3.3.1 Norwegian Earth System Model (NorESM)

NorESM is a numerical model built of four individual but interactive land, atmosphere, ocean and ice modules (Bentsen et al. 2013, Iversen et al. 2013). NorESM takes into account climate effects of organic, black carbon, sulphate, dust, and sea salt aerosols. The aerosol description is based on production-tagged mass concentrations, internally or externally mixed, described explicitly for each of the different modes of the aerosol size distribution (nucleation, Aitken, accumulation, and coarse mode). Aerosol microphysical properties such as effective dry particle size and aerosol optical parameters, including the effect of hygroscopic growth, are estimated by use of interpolations in pre-calculated look-up tables which take ambient RH and a range of process-specific aerosol concentrations from the model as input parameters. Aerosol hygroscopic growth for RH < 100% is estimated using similar look-up tables. Activation of aerosol particles acting as CCN follows the approach of Abdul-Razzak and Ghan (2000) and the cloud microphysics are simulated with a two-moment scheme. Aerosol direct and indirect effects on the Earth's radiation budget may be estimated individually via parallel calls to the radiative transfer code. The model sensitivity of hygroscopicity was studied both with and without interactions between aerosols and meteorological conditions, named here as online and offline calculations, respectively (see Table S4 in Paper IV for a list of simulations). The model was set up with a horizontal resolution of 1.9° x 2.5° and 26 levels in the vertical. The model was run for 7 years in offline mode with 2 years spin-up and 22 years in online mode with 7 years spin-up.

#### 3.3.3.2 ECHAM6-HAM2 model

ECHAM-HAMMOZ (version echam 6.1- ham2.2-moz0.9), referred to as ECHAM6-HAM2 is a global aerosol-chemistry climate model. The aerosol-cloud-climate interactions are based on the aerosol module HAM2 (Zhang et al., 2012) coupled to the atmospheric general circulation model ECHAM6 (Stevens et al., 2013). HAM2 uses the two-moment M7 modal aerosol microphysics scheme (Vignati et al., 2004) and a two-moment cloud microphysics scheme that includes prognostic equations for the cloud droplet and ice crystal number concentrations as well as cloud water and cloud ice (Lohmann and Hoose, 2009). The activation of aerosol particles into cloud droplets is parameterised according to Barahona et al. (2010). HAM2

calculates the global evolution of five aerosol species: sulphate, organic matter, black carbon, sea salt, and dust. These species are the constituents of both internally and externally mixed aerosol particles whose size distribution is represented by seven unimodal log-normal distributions. These seven modes describe four size classes (nucleation, Aitken, accumulation and coarse) and two hygroscopic classes (hydrophobic and hydrophilic). Simulations were performed at 1.9° × 1.9° spectral resolution using 31 vertical levels. The model was run for two 5-year present-day (years 2006-2010) with one month spin-up.

# 4. Results and discussion

## 4.1 Hygroscopic behavior of secondary organic aerosols (SOA)

The comparison between the SBS model and the complete dissolution assumption demonstrated a systematic under-prediction (up to 40%) of the activation diameter by the complete dissolution model. The κ and ε -based solubility models, on the other hand, were generally within 10% (in most cases within 5%) of the activation diameter predicted using the full solubility distribution representation, Fig. 7. The simplified κ and ε models gave a satisfactory representation of the activation diameter for a given supersaturation, although the fitted soluble fraction ε or hygroscopicity parameter κ obtained for a given mixture did not seem to reflect the average solubility of the mixture. Instead, they were related to the fraction of the mixture with solubility exceeding 10 g $L^{-1}$ for the ideal mixture and 1 g $L^{-1}$ for the unity activity assumptions. Our results suggest that the critical range for limited solubility in CCN activation is between 0.1-100 g $L^{-1}$ and in most cases material below 1 g $L^{-1}$ is practically insoluble and material above 10 g $L^{-1}$ completely soluble. Our values for the limiting solubilities for complete dissolution are in agreement with the values of 3 g $L^{-1}$ and 1 g $L^{-1}$ previously reported by Huff Hartz et al. (2006) and Chan et al. (2008) based on experimental data on specific mixtures.

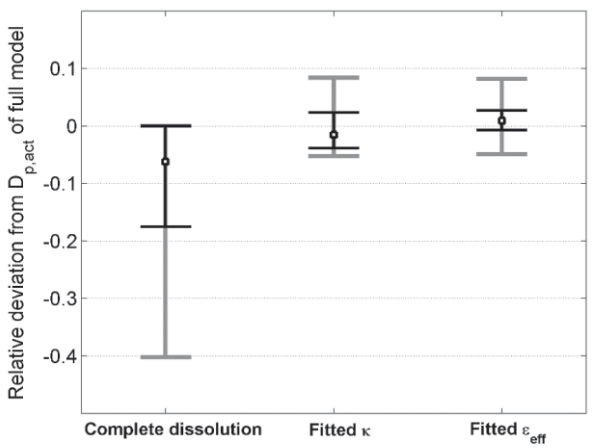


Figure 7: The performance of the simplified solubility representations in predicting the activation diameter for a given supersaturation as compared with the SBS model. The black bars depict the 25- and 75-percentiles and the gray bars the 10- and 90-percentiles.

In Paper III, the water uptake behavior of biogenic SOA particles formed from isoprene ($C_5H_8$), α-pinene ($C_{10}H_{16}$), and longifolene ($C_{15}H_{24}$) precursors were investigated. In figure 8, the hygroscopic growth factor (HGF), particle bounced fraction (BF), the hygroscopicity parameter ($\kappa$) and the oxidation state (oxygen-to-carbon ratio, O:C) of these SOA particles are shown. We deduced that the particles with BF > 0 are solid or semisolid, and that the particles with BF = 0 behave mechanically as liquids (Virtanen et al., 2010).

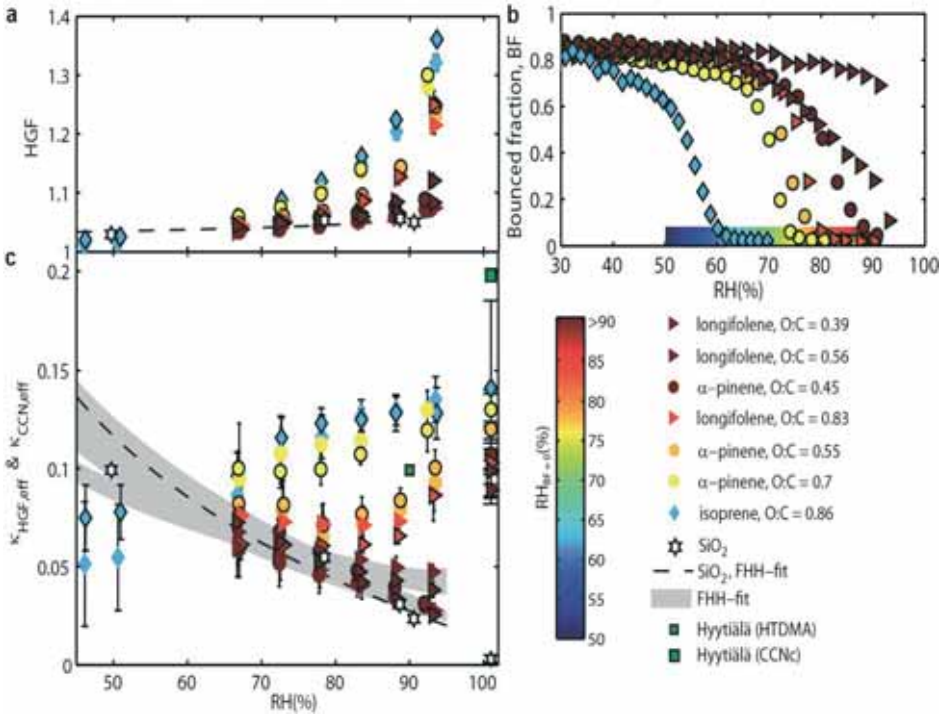


Figure 8: Hygroscopic behavior of laboratory generated SOA particles described using results from HTDMA, CCNc and ABI measurements. Spheres represent α-pinene, triangles longifolene and diamonds isoprene SOA particles. Panel a shows the measured HGFs as a function of RH. Mobility diameters, $d_p$, of the SOA particles, 50 nm (without edge color) and 100 nm (black edges), and 50 nm for $SiO_2$ (white stars), are plotted. The colors of the data points represent the RH values where the bounced fractions falls to zero as shown in panel b (i.e. for isoprene the zero point is RH ~ 62% whereas for α-pinene with lowest O/C the zero point is RH ~ 92%). Panel c shows the hygroscopicity parameters calculated from HTDMA and CCNc data, the gray area represents FHH isotherms fit to the data, and the green rectangles represent ambient data ($d_p$ = 100 nm) measured in spring 2012 at the SMEAR II station in Hyytiälä, Finland (Sect. 3.2.1.2). Error estimates for ambient $\kappa_{HGF,eff}$ and $\kappa_{CCN,eff}$ are ±0.03 and ±0.04, respectively.

To relate HGF to phase state, symbols in Fig. 8a and 8b are colored by the RH at which BF approached 0. SOA particles that attain BF = 0 at RH > 90% have the smallest HGF values. SOA particles that attain BF = 0 at RH = 61–72% have the highest HGF values. Figure 8c further shows that for less-oxidized, semisolid α-pinene SOA (O:C = 0.45) and longifolene SOA (O:C = 0.39 to 0.56), $\kappa$ decreases with increasing RH. The same behavior was observed for $SiO_2$ particles, which can take up water only via surface adsorption. This suggests that a similar mechanism occurs for semisolid or sparingly soluble SOA particles, where the apparent hygroscopic growth is due to surface adsorption of water rather than bulk water uptake. The adsorption behavior can be quantified in the subsaturated regime using FHH adsorption theory (Adamson and Gast, 1997; Sorjamaa and Laaksonen 2007). Isoprene SOA and highly-oxidized α-pinene SOA (O:C = 0.7), exhibit a increase of $\kappa$ with increasing humidity. Having a low BF in the lower range of RH (61–72%), indicates that these SOA particles liquefy at lower water activities because they consist of compounds having higher solubility. For α-pinene SOA with O:C = 0.55 and longifolene SOA with O:C = 0.83, an intermediate trend is observed. First, κ decreases with increasing humidity up to about 80% and then increases with increasing RH. This behavior suggests a transition from adsorption to a dissolution-dominated process.

In Paper IV, we tried to reproduce the data represented for two of these SOA types, one formed from isoprene (IP, O:C = 0.86) and the other one from α-pinene (MT, O:C = 0.45) precursors by using the solubility distributions of IP and MT SOA (Sect. 3.2.2.1 and Fig. 5) in the SBS model. Figure 9 shows that the SBS model (simple model, just dissolution) cannot explain the hygroscopic behavior of these SOA. In our first alternative approach, we coupled the SBS model with treatment of adsorption theory. We did the calculations for both ideal ($\Gamma_w$=1) and nonideal ($\Gamma_w$ = calculated) mixtures. The SBS model plus adsorption, i.e. considering the nonideality, showed better agreement with observation data for MT compared with IP, see the orange line in Fig. 9. In our second more comprehensive approach, we used the AIOMFAC + EVAPORATION model, which takes into account the nonideality of the mixture, a potential liquid-liquid phase separation, coupled gas-particle partitioning of semivolatile organic vapors and water, and a mass transfer correction for semisolid organic particles at low RH. The results from this model are shown as blue lines in Fig. 9. Gas-particle partitioning showed a more significant change in results for IP-SOA with more semivolatile compounds compared with MT-SOA. The laboratory results for IP and MT are consistent with values measured at the Southern Oxidant and Aerosol Study (SOAS) campaign in Alabama, US (VOC profile dominated by IP) and the SMEAR II station in Hyytiälä, Finland (VOC profile dominated by MT), respectively (Sect. 3.2.1.2).

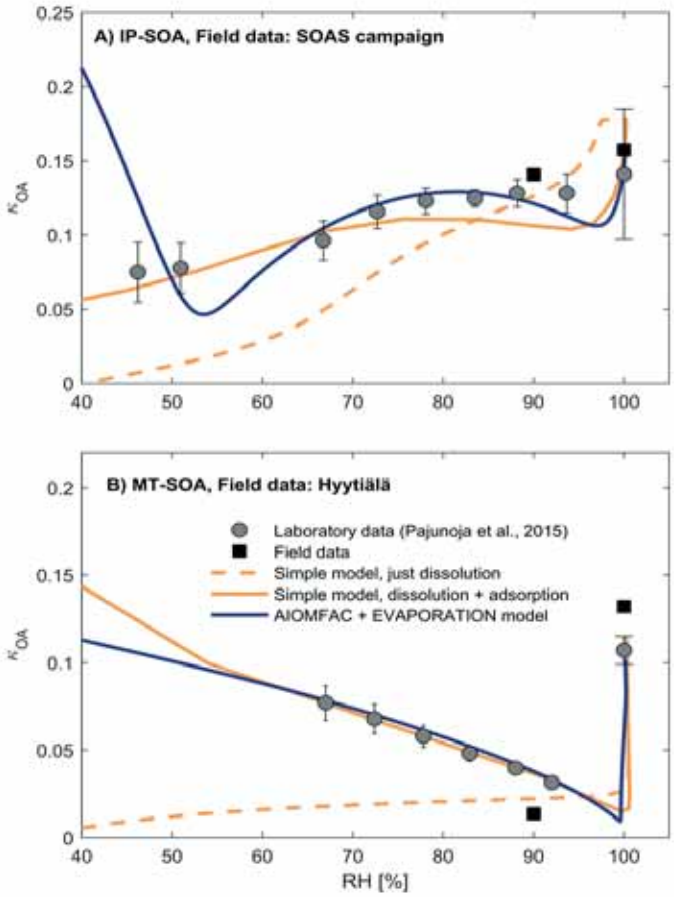


Figure 9: The RH-dependences of the hygroscopicity parameter $\kappa_{OA}$ for isoprene- and monoterpene-derived SOA. A) The hygroscopicity parameter $\kappa_{OA}$ for laboratory-generated 100 nm particles from IP photo-oxidation (grey points, O:C = 0.89, Paper III), organic aerosol sampled at the SOAS site in Alabama (black squares, O:C = 0.63 ± 0.06), and as predicted using two state of the art thermodynamic models (SPARC and AIOMFAC). The SPARC equilibrium calculations are presented for a case accounting for the solubility of the SOA components only (dashed orange lines) as well as a case including also treatment of adsorptive water uptake and non-ideality of the aqueous phase (orange line). The AIOMFAC + EVAPORATION calculations account for mixture non-ideality, a potential liquid-liquid phase separation, coupled gas-particle partitioning of semi-volatile organic vapors and water, and a mass-transfer correction for semi-solid organic particles at low RH (blue line). B) As A but for MT ozonolysis SOA (grey points, O:C = 0.56, Paper III) and organic aerosol sampled at the SMEAR II station in Hyytiälä, Finland (black squares, O:C = 0.63 ± 0.06).

Previous laboratory data indicate that the κ parameters measured for organic aerosols can vary substantially comparing sub and super-saturated conditions (Prenni et al., 2007; Wex et al., 2009; Hodas et al., 2016). On the other hand, there is only a minor discrepancy between sub- and super-saturated RH for inorganics (Petters and Kreidenweis, 2007). In Figure 8, the difference between $\kappa$ at subsaturation ($\kappa_{HGF}$) and supersaturation ($\kappa_{CCN}$) for SOA particles ($\Delta\kappa_{OA}$) is shown. $\Delta\kappa_{OA}$is smallest for particles that dissolve at lower RH and have a higher O:C and largest for particles with smaller O:C values with adsorptive behavior (Paper III). This discrepancy is also evident in Fig. 9, comparing IP and MT-SOA and the field data (Paper IV). We suggest that this discrepancy is related to the solubility and phase state. As the oxidation state (O:C) of SOA compounds increases (e.g. due to chemical aging), their solubility also increases due to an increasing number of polar functional groups. This results in an increase in $\kappa_{HGF}$ of the mixture and a decrease in $\Delta\kappa_{OA}$. To investigate this discrepancy with respect to phase state, we looked into the optical microscopy images of super-micron samples of MT and IP derived SOA (Fig. 10).

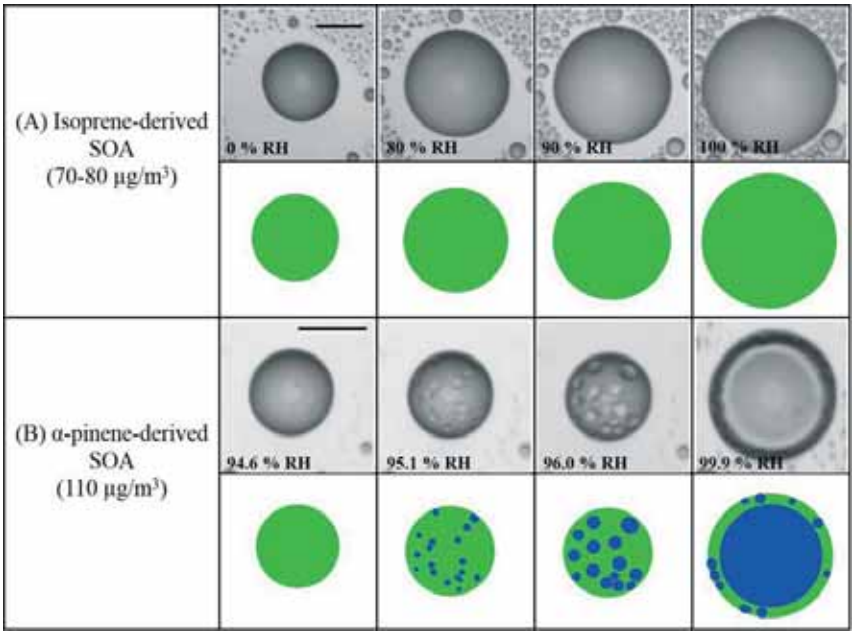


Figure 10: Optical images of micrometer scale SOA particles with increasing relative humidity. (A) isoprene-derived SOA for the mass concentrations of 70 - 80 µg $m^{-3}$ and (B) α-pinene-derived SOA for the mass concentrations of 110 µg $m^{-3}$ (Panel B was reproduced from Renbaum-Wolff et al., 2016). Note that the light gray circles at the center of the particles is an optical effect due to the hemispherical nature of the particle. Illustrations are shown below the images for clarity. Green: organic-rich phase. Blue: water-rich phase. The scale bar is 20 µm.

For the MT-SOA, a single organic-rich phase was observed at < 95 % RH, but at about 95 % RH, liquid-liquid phase separation occurred to form two phases: an organic-rich and water-rich phase (Fig. 10B). In contrast to MT-SOA, IP-SOA showed only one phase over the entire RH range (Fig. 10A). Our previous model approaches indicate, in line with the microscopy images, that the key process explaining the large $\Delta\kappa_{OA}$ in the case of the MT system is the formation of a new aqueous phase in the particles between 90 and 100% RH. As RH increases further, the aqueous phase volume increases with the fraction of OA dissolved. At supersaturation both IP and MT derived SOA behave as nearly completely soluble in water, as indicated by high $\kappa_{OA}$ values observed. These results suggest that the observed $\Delta\kappa_{OA}$ between 90% RH and supersaturation can be reproduced if the phase separation effects are considered.

### 4.2 Coupled hygroscopicity and radiative transfer model

The scattering and absorption of incoming solar radiation is dependent on the size and chemical composition of the aerosol which can be altered through the uptake of water by the aerosol particles. To improve our understanding of the role of water and aerosols in the global climate system we need to expand our knowledge about these interactions. In Paper I we focused on the impact of water uptake by aerosol particles on their optical properties and Aerosol Direct Radiative Effect (ADRE) in the Arctic environment at Zeppelin station in Ny-Ålesund, Svalbard. The performance of the coupled hygroscopicity and radiative transfer model was evaluated by comparing the results with direct measurements of growth factors (GF) and scattering coefficients ($\sigma_{sp}$), which were available for parts of the year 2008 (Silvergren et al., 2014; Zieger et al., 2010). The calculated GF showed a very good agreement with the measurements for autumn and early winter (September–January) with predicted values within about 2 % of the measurements, but a positive bias of 4–15 % for spring and summer (February–August). The modeled and measured dry scattering coefficients ($\sigma_{sp,dry}$) showed a good agreement ($R^2$ = 0.95). For most of the days the modeled scattering coefficients were within 20 % of the measured values. The calculated and modeled wet scattering coefficients ($\sigma_{sp,wet}$) also showed a reasonable agreement with the experiments as well ($R^2$=0.64). For most of the days the deviation between the modeled and measured scattering coefficient was less than 40 %. With the coupled model, we were able to use long term dry size distribution data recorded continuously at the Zeppelin station since year 2000 (Tunved et al., 2013), focusing on year 2008. One of the advantages of using the long-term measurements was the possibility to investigate the seasonal variation of hygroscopic growth, optical properties and direct radiative effect of aerosol particles. The ambient aerosol scattering coefficients at the surface showed a clear seasonal variation with the highest

values during the haze period (March-April-May) and the lowest values during summer (June-July). The results showed a significant impact of hygroscopic growth on aerosol optical properties and ADRE. For instance the annual averaged enhancement factor $f$ (RH), which is the ratio of humidified scattering coefficient and dry scattering coefficient, was about 4.30±2.26. $f$ (RH) was largest during summer and fall and smallest during the haze period in spring. The ambient RH was found to be the most important factor determining the ambient GF and $f$ (RH) as compared with the aerosol particle dry size and composition. In most cases, the deviation of the aerosol scattering coefficient was less than 5 % when assuming a composition of pure ammonium sulphate instead of using chemical composition statistics based on the filter measurements. The seasonal behavior of the ADRE showed a different pattern as compared to the scattering coefficients at the surface: the most negative values (i.e. the largest cooling effect) were found during July, August and September. Including the hygroscopic growth of aerosol particles increased the predicted ambient Aerosol Direct Radiative Effect (ADRE) with a factor of about 1.6 to 3.7 compared to the dry ADRE, depending on the season Fig. 11.

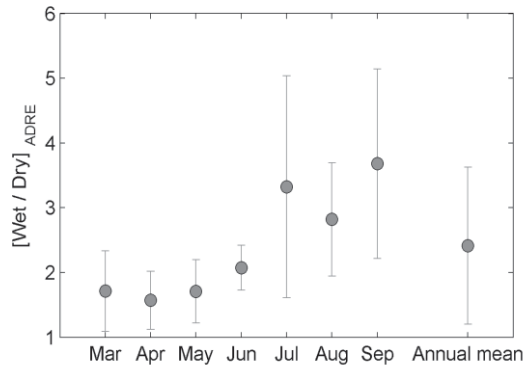


Figure 11: The ratio between Wet and Dry aerosol direct radiative effect ADRE. The error bars indicate the standard deviations. For the Wet case we used ambient RH in the model and for the Dry case RH=0 in the model (GF=1). For the months not shown, the ADRE was assumed to be zero due to lack of sunlight.

In most atmospheric models a single-parameter hygroscopicity framework based on $\kappa$ is used to describe the aerosol interaction with water vapor. In these models only one $\kappa$ value, i.e. either $\kappa_{CCN}$ or $\kappa_{HGF}$ is used in both sub- and supersaturation regimes. Fig (12, left panel) shows the calculated ADRE using the coupled hygroscopicity and radiative transfer model for different $\kappa_{HGF}$ and $\kappa_{CCN}$, measured in Hyytiälä forest. In Fig (12, right panel) the relative change in ADRE if $\kappa_{CCN}$ is employed in the calculation instead of $\kappa_{HGF}$ for a case study representing the conditions in boreal forest during spring (composition dominated by SOA ~ 80%) is shown. The median

relative change in the ADRE is of the order of 15% (the quartiles being at about 7% and 32%). Our results show that using one single $\kappa$ for both sub- and supersaturation regimes will introduce uncertainties to aerosol direct radiative calculations.

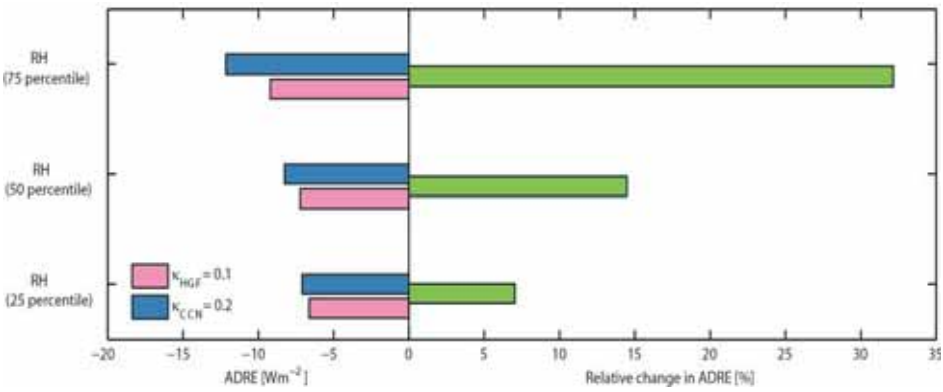


Figure 12: Comparison of simulated Aerosol Direct Radiative Effect (ADRE) predicted from measured hygroscopicity κ values in Hyytiälä forest. ADREs [Wm$^{-2}$] calculated by the SBDART-model are shown in the left panel for two different total $\kappa$ values measured in the campaign ($\kappa_{HGF}$ = 0.1 and $\kappa_{CCN}$ = 0.2, respectively). Relative change in ADRE [%] between the two simulations is shown in the right panel.

### 4.3 Sensitivity of global climate models to treatment of water uptake of organic aerosols

Previous studies have suggested that the water-affinity of SOA plays a minor role in determining the climate impact of these particles (Morales Betancourt and Nenes, 2014). Our results from Paper IV shows that the picture is somewhat more complex than this. In Paper IV, we used two climate models, NorESM and ECHAM6-HAM2, to study the sensitivity of the Earth's radiative budget to assumptions about organic aerosol hygroscopicity and CCN activity. Both models represent OA with one hygroscopicity value for both sub- and supersaturation. These two model differ significantly in their overall OA mass concentration, NorESM has a global average OA loading of about 3.8 Tg, while ECHAM6-HAM2 has a global average OA loading of about 0.8 Tg. NorESM simulates a global average difference of about -1.02 W m$^{-2}$ in aerosol radiative effects, using $\kappa_{OA}$values of 0.15 and 0.05. ECHAM6-HAM2, on the other hand, simulates about one fourth of the NorESM sensitivity to $\kappa_{OA}$ (difference of -0.25 W m$^{-2}$). The magnitude of the sensitivity is probably driven by the overall OA loading present in the model. The sensitivity in both models is highly regional, being most pronounced over tropical regions (Figs. 13a and b), and the effects of $\kappa_{OA}$

are largest for RHs over 60%. The indirect effect of aerosol particles dominates the sensitivity in both models as compared to the direct effect. These results suggest that representing all OA with one constant hygroscopicity parameter can introduce significant uncertainties in calculating the climate impacts of organic aerosol particles in global models and constraining the OA water-affinity might be more important than previously thought.

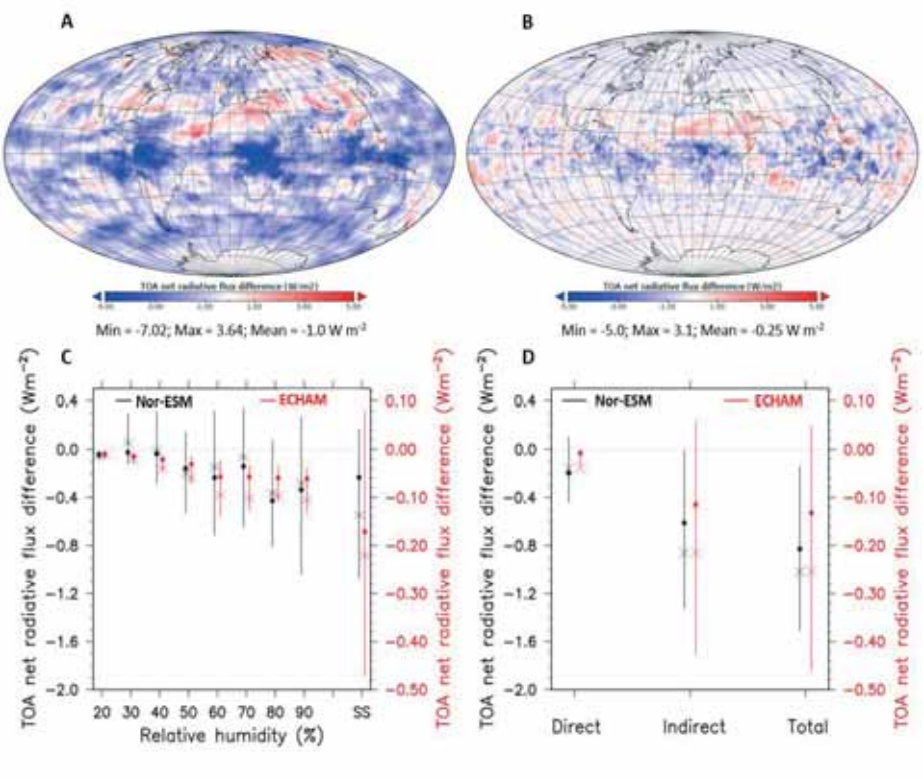


Figure 13: Sensitivities of two climate models to $\kappa_{OA}$. A) Difference in the top-of-the-atmosphere (TOA) radiative flux in NorESM model simulations of the present-day atmosphere (22 years simulated) for $\kappa_{OA}$ varying between 0.05 and 0.15. B) Difference in the top-of-the-atmosphere (TOA) radiative flux in the ECHAM6-HAM2 model simulations (7 years simulated) of the present-day atmosphere for $\kappa_{OA}$ varying between 0.05 and 0.15. C) TOA radiative flux difference for $\kappa_{OA}$ varying between 0.05 and 0.15 as a function of RH for NorESM (left axis, black symbols) and ECHAM (right axis, red symbols). Only gridpoints over land and outside of the polar regions have been considered. D) The contribution of the direct vs. indirect aerosol effects to the model sensitivity for NorESM (left axis, black symbols) and ECHAM (right axis, red symbols).

# 5. Conclusions

In the following section, I aim to answer the research questions defined in the beginning of this thesis (Sect. 1.4).

**A) Investigating the links between aerosol molecular composition, hygroscopic growth and CCN activation, with a focus on organic compounds**.

(1) We found that in regions where the composition of aerosols is dominated by inorganics (e.g. the Arctic), the hygroscopic behavior of aerosols is controlled by solubility and well represented with simple aerosol models. Highly soluble inorganics are able to make a diluted aqueous phase over the entire RH range, starting from low RH values. A more complex hygroscopic behavior was detected in regions where the composition of aerosols is dominated by organics (e.g. boreal forests). Organics consist of thousands of different compounds with different solubilities. Due to this complexity, the processes governing their hygroscopic behavior is more difficult to represent compared with inorganics. We found that solubility limitations to a large extent govern the hygroscopic and CCN behavior of low-soluble MT-SOA. Model estimates applying limited solubility assumptions coupled with treatment of adsorption, could reproduce the laboratory derived data for IP and MT-SOA with good agreement. However, constraining the theoretical models of the hygroscopic growth to match experimental data thus becomes increasingly challenging at subsaturation, requiring consideration of coupled bulk to surface partitioning, gas-particle partitioning of the semivolatile vapors and nonideality of the liquid phases. On the other hand at supersaturation, both IP and MT-derived SOA behave as nearly completely soluble in water.

(2) The single-parameter hygroscopicity framework is based on κ-Köhler theory, where the hygroscopicity parameter, κ, represents a quantitative measure of aerosol water uptake characteristics and CCN activity. If a single κ can be assumed to represent a given mixture, the value should naturally be the same in both the subsaturated ($\kappa_{HGF}$) and supersaturated ($\kappa_{CCN}$) regimes. However, results from laboratory studies show discrepancy between $\kappa_{HGF}$ and $\kappa_{CCN}$ for some organic compounds. The findings presented in this thesis suggest that this difference is related to both solubility and phase state. Results from optical microscopy images show below 95% RH, MT-SOA has a single organic-rich phase but at ~95% RH, liquid-liquid phase separation occurred to form two phases: an organic-rich and a water-rich phase. For IP-

SOA, one single phase was observed over the entire RH range. This can explain the high $\Delta\kappa_{OA}$ for MT-SOA and the low $\Delta\kappa_{OA}$ for IP-SOA. On the other hand, as the oxidation state (O: C) of SOA compounds increases, their water solubility also increases, resulting in a higher $\kappa_{OA}$ below 95% RH and a lower $\Delta\kappa_{OA}$ in response.

**B) Testing simplifying approaches for describing water uptake, CCN activation and their impact on radiative properties.**

(1) We applied the coupled hygroscopicity and radiative transfer model for the Artic environment, using observational data including number size distribution, chemical composition and RH collected at the Zeppelin research station in Ny-Ålesund, Svalbard for the year 2008. The comparison between our results from the coupled hygroscopicity and radiative transfer model to the short-term campaigns for growth factors and scattering coefficients showed a good agreement, which indicates that the coupled hygroscopicity and radiative transfer model is a reliable tool to be used also in other regions dominated by well-understood inorganic species. We found that calculated aerosol effects on the radiative budget are strongly dependent on how we represent the interactions between aerosol particles and water vapor. The hygroscopic growth of aerosol particles in the ambient Arctic atmosphere enhance the aerosol scattering coefficients with a factor of $4.30 \pm 2.26$ (mean $\pm$ standard deviation), and increase the predicted ambient aerosol direct radiative effect with a factor of about 1.6 to 3.7 compared to completely dry aerosols. The ambient RH was found to be the most important factor determining the hygroscopic growth and its impact on aerosol optical properties as compared with the aerosol particle dry size and composition.

(2) With the Solubility Basis Set (SBS), we described the complexity of organic mixtures with different solubilities as a continuous solubility distribution. Comparison between SBS model and simplified models showed that describing the mixture with single hygroscopicity parameter $\kappa$ and $\varepsilon$ depends on the solubility distributions. The $\varepsilon$ and $\kappa$ values describing the CCN activation of the investigated theoretical mixtures were found to correspond to the fraction of material with solubilities larger than a given threshold solubility $c_t$ , which depends on the assumptions of organic compounds interactions. $c_t$ is about 10 g $L^{-1}$ for ideal mixture (where organics limit each other's dissolution) and 1 g $L^{-1}$ for the unity activity (where organics behave as pure compounds and do not influence each other's dissolution). Our results suggest that the critical range for limited solubility in CCN activation is between 0.1-100 g $L^{-1}$ and in most cases material below 1 g $L^{-1}$ is practically insoluble and material above 10 g $L^{-1}$ completely soluble.

(3) The single-parameter hygroscopicity framework is commonly used in numerical models to quantify the climate effects of aerosol particles. In these models the same κ value is used for both sub and super-saturated regimes. We showed that for a case study representing boreal forest conditions in box/column model, where aerosol composition is dominated by SOA, if $\kappa_{CCN}$ is employed in the calculations instead of $\kappa_{HGF}$, the median relative change in aerosol direct radiative effect is of the order of 15%. We also found that representing all OA with one constant hygroscopicity parameter can introduce significant uncertainties in determining the climate impact of OA in global models. For instance, the NorESM and ECHAM6_HAM2 models simulate a global average difference of about -1.02 $Wm^{-2}$ and -0.25 $Wm^{-2}$ in aerosol radiative effects between cases with $\kappa_{OA}$ values of 0.15 and 0.05. In contrast with previous studies, our results indicate that the water affinity of organics can play a major role in determining the climate effect of these particles, depending on the way these molecular interactions are treated.

# 6. Outlook

In this thesis work, new tools and frameworks for investigating the hygroscopicity and CCN activation behavior of aerosol particles have been developed. The coupled hygroscopicity and radiative transfer model developed in Paper I can be applied to fill the gap between the dry particle size distributions and the wet ambient optical properties to explore the effect of humidity on ADRE at different sites or conditions. For instance, we have used the model to reconcile the differences between in-situ and remote sensing observations of aerosol optical properties (Tesche et al., 2014). The Solubility Basis Set (SBS) developed in Paper II was used in Paper IV along with a treatment of adsorption to describe the water uptake and CCN activation behavior of IP- and MT-SOA. In addition to this approach we assumed a more comprehensive treatment which takes into account the gas-particle partitioning of the semivolatile vapors and Liquid-Liquid Phase Separation (LLPS) effects. We also tested the sensitivity of climate forcing reproduced by two global models to the water affinity of OA. We found that the currently used single-parameter hygroscopicity framework in global models can introduce significant errors in quantifying the climate effect of organic aerosols. Instead, a self-consistent representation of the climate impacts of OA should rely on an oxidation-state-dependent water-affinity approach, and ideally this approach would be coupled to both surface phenomena and a dynamically evolving volatility representation. A future study comparing other global models and their sensitivities to organic water uptake assumptions will be beneficial to estimate the importance of reconsidering organic aerosols with more detailed microphysics in global models. Although this study helped to better understand the aerosol-water interaction in general and also how to explain the discrepancy between sub and super-saturated conditions, there is still much to learn about organic-water interaction and their role in climate.

# 7. Acknowledgement

Firstly I would like to thank my supervisors, Ilona Riipinen, Annica Ekman, and Peter Tunved who were always there for me. Special thanks to my main supervisor Ilona Riipinen for her continuous support and for giving me the chance to work at the warm and friendly environment of ACES. Finally I would like to thank all my friends and colleagues at ACES for their help, support and understanding.

I would like to thank:

- The Norwegian Institute for Air Research (NILU)
- The Alfred Wegener Institute (AWI)
- The Swedish Environmental Protection Agency
- The Nordic Centre of Excellence CRAICC (Cryosphere-Atmosphere Interactions in a Changing Arctic Climate)
- Vetenskapsrådet (grant 2011-5120)
- The European Research Council (StG-278277 ATMOGAIN)
- The Swedish Research Council Formas (2015-749)
- Knut and Alice Wallenberg Foundation (Wallenberg Fellowship AtmoRemove)
- Academy of Finland (grants 272041 and 259005)
- The Natural Environment Research Council (NERC grant)
- The Norwegian Research Council (EVA grant no. 229771)
- The Natural Sciences and Engineering Research Council of Canada (RGPIN/04315-2014)
- United States National Science Foundation (ATM-1242258, AGS-1242932, AGS 1360834)
- United States Environmental Protection Agency (STAR Grant R835410)
- National Oceanic and Atmospheric Administration (CPO Award 538NA10OAR4310102)
- Electric Power Research Institute (10004734)
- US Department of Energy (BER/ASR DE-SC0016559, DE-SC0012792)
- Georgia Institute of Technology and the Nordic Centre of Excellence eSTICC
- The Swedish National Infrastructure for Computing (SNIC)
- The Norwegian meteorological institute (Met.no).

# References


Aas, W., Solberg, S., Manø, S. og Yttri, K.E.: Overvåking av langtransportert forurenset luft og nedbør. Atmosfærisk tilførsel, 2008. Norsk institutt for luftforskning, Kjeller, OR 22/2009 (SFT (Klif) rapport nr 1051/2009), 2009.

Abdul-Razzak, H. and Ghan, S. J.: A parameterization of aerosol activation: 2. Multiple aerosol types, J. Geophys. Res., 105(D5), 6837–6844, doi:10.1029/1999JD901161, 2000.

Adamson, P., and Gast, A.: Physical Chemistry of Surfaces, 6th ed., Wiley Interscience, New York, 1997.

Aiken, A.C., Decarlo, P. F., Kroll, J. H., Worsnop, D.R., Huffman, J. A., Docherty, K. S., Ulbrich, I. M., Mohr, C., Kimmel, J. R., Sueper, D., Sun, Y., Zhang, Q., Trimborn, A., Northway, M., Ziemann, P.J., Canagaratna, M. R., Onasch, T.B., Alfarra, M.R., Prevot, A. S. H., Dommen, J., Duplissy, J., Metzger, A., Baltensperger, U. and Jimenez, J. L.: O/C and OM/OC ratios of primary, secondary, and ambient organic aerosols with high-resolution time-of-flight aerosol mass spectrometry, Environ. Sci. Technol. 42(12), 4478-4485, 2008.

Albrecht, B. A.: Aerosols, Cloud Microphysics, and Fractional Cloudiness, Science (80)., 245(4923), 1227–1230, 1989.

Andrews, E. and Larson, S. M.: Effect of surfactant layers on the size changes of aerosol particles as a function of relative humidity, Environ. Sci. Technol., 27(5), 857–865, doi:10.1021/es00042a007, 1993.

Ansari, A. S. and Pandis, S. N.: Prediction of multicomponent inorganic atmospheric aerosol behavior, Atmos. Environ, 33, 1999.

Asa-Awuku, A. and Nenes, A.: Effect of solute dissolution kinetics on cloud droplet formation: Extended Köhler theory, Geophys. Res., 112, D22201, doi:10.1029/2005JD006934, 2007.

Asa-Awuku, A., Nenes, A., Gao, S., Flagan, R. C and Seinfeld, J. H.: Water-soluble SOA from alkene ozonolysis: composition and droplet activation kinetics inferences from analysis of CCN activity, Atmos. Chem. Phys., 10, 1585–1597, 2010.

Barahona, D., West, R. E. L., Stier, P., Romakkaniemi, S., Kokkola, H. and Nenes, A.: Comprehensively accounting for the effect of giant CCN in cloud

activation parameterizations, Atmos. Chem. Phys., 10, 2467-2473, doi:10.5194/acp-10-2467-2010, 2010.

Bentsen, M., Bethke, I., Debernard, J.B., Iversen, T., Kirkevåg, A., Seland, Ø., Drange, H., Roelandt, C., Seierstad, I.A., Hoose, C. and Kristjánsson, J. E.: The Norwegian Earth System Model, NorESM1-M. Part 1: Description and basic evaluation, Geosci. Model Dev., 6, 687-720, doi: 10.5194/gmd-6-687-2013, 2013.

Bertram, A. K., Martin, S. T., Hanna, S. J., Smith, M. L., Bodsworth, A., Chen, Q., Kuwata, M., Liu, A., You, Y. and Zorn, S.R.: Predicting the relative humidities of liquid-liquid phase separation, efflorescence, and deliquescence of mixed particles of ammonium sulfate, organic material, and water using the organic-to-sulfate mass ratio of the particle and the oxygen-to-carbon elemental ratio of the organic component, Atmos. Chem. Phys., 11, 10995-11006, doi:10.5194/acp-11-10995-2011, 2011.

Canagaratna, M. R., Jimenez, J. L., Kroll, J. H., Chen, Q., Kessler, S. H., Massoli, P., Hildebrandt Ruiz, L., Fortner, E., Williams, L. R., Wilson, K. R., Surratt, J. D., Donahue, J. T., Jayne, N. M. and Worsnop, D. R.: Elemental ratio measurements of organic compounds using aerosol mass spectrometry: characterization, improved calibration, and implications, Atmos. Chem. Phys., 15, 253-272, doi:10.5194/acp-15-253-2015, 2015.

Chan, M. N., Kreidenweis, S. M., and Chan, C. K.: Measurements of the hygroscopic and deliquescence properties of organic compounds of different solubilities in water and their relationship with cloud condensation nuclei activities, Environ. Sci. Technol. 42 3602–3608, 2008.

Charlson, R. J. and Pilat, M. J.: Climate: The Influence of Aerosols, J. Appl. Meteorol., 8(6), 1001–1002, doi:10.1175/1520-0450(1969)008<1001:CTIOA>2.0.CO;2, 1969.

Charlson, R. J., Schwartz, S. E., Hales, J. M., Cess, R. D., Coakley, J. A., Hansen, J. E. and Hofmann, D. J.: Climate Forcing by Anthropogenic Aerosols, Science, 423–430, 1992.

Chen, Q., Liu, Y., Donahue, N. M., Shilling, J.E. and Martin, S. T.: Particle-phase chemistry of secondary organic material: modeled compared to measured O:C and H:C elemental ratios provide constraints. Environ. Sci. Technol., 45(11), 4763-4770, 2011.

Coakley, J. A., Cess, R. D. and Yurevich, F. B.: The Effect of Tropospheric Aerosols on the Earth's Radiation Budget: A Parameterization for Climate Models, J. Atmos. Sci., 40(1), 116–138, doi:10.1175/1520-0469(1983)040<0116:TEOTAO>2.0.CO;2, 1983.

Compernolle, S., Ceulemans, K. and Müller, J. F. : EVAPORATION: a new vapor pressure estimation method for organic molecules including non-

additivity and intramolecular interactions, Atmos. Chem. Phys., 11, 9431-9450, doi:10.5194/acp-11-9431-2011, 2011.

Cruz, C. N. and Pandis, S. N.: Deliquescence and Hygroscopic Growth of Mixed Inorganic - Organic Atmospheric Aerosol, Environ. Sci. Thecnol., 34(20), 4313–4319, 2000.

Farmer, D. K., Cappa, C. D., and Kreidenmweis, S. M.: Atmospheric processes and their controlling influence on cloud condensation nuclei activity, Chem. Rev., 115, 4199–4217, doi:10.1021/cr5006292, 2015.

Fierz-Schmidhauser, R., Zieger, P., Wehrle, G., Jefferson, A., Ogren, J., Baltensperger, U., and Weingartner, E.: Measurement of relative humidity dependent light scattering of aerosols, Atmos. Meas. Tech., 3, 39–50, doi:10.5194/amt-3 39-2010, 2010.

Finessi, E., Decesari, S., Paglione, M., Giulianelli, L., Carbone, C., Gilardoni, S., Fuzzi, Saarikoski, S., Raatikainen, T., Hillamo, R., Allan, J., Mentel, TH. F., Tiitta, P., Laaksonen, A., Petäjä, T., Kulmala, M., Worsnop, D. R. and Facchini, M. C.: Determination of the biogenic secondary organic aerosol fraction in the boreal forest by NMR spectroscopy, Atmos. Chem. Phys., 12, 941-959, doi:10.5194/acp-12-941-2012, 2012.

Fitzgerald, J. W., Hoppel, W. A. and Vietti, M. A.: The Size and Scattering Coefficient of Urban Aerosol Particles at Washington, DC as a Function of Relative Humidity, J. Atmos. Sci., 39(8), 1838–1852, doi:10.1175/1520-0469(1982)039<1838:TSASCO>2.0.CO;2, 1982.

Frenkel, J.: Kinetic theory of liquids, pp. 332–339, Oxford University Press, 1946.

Goldstein, A., and Galbally, I.: Known and unexplored organic constituents in the Earth's atmosphere, Environ. Sci. Technol., 40(5), 1514 – 1521, 2007.

Guenther, A. B., Jiang, X., Heald, C. L., Sakulyanontvittaya, T., Duhl, T., Emmons, L. K., and Wang, X.: The Model of Emissions of Gases and Aerosols from Nature version 2.1 (MEGAN2.1): an extended and updated framework for modeling biogenic emissions, Geosci. Model Dev., 5, 1471-1492, https://doi.org/10.5194/gmd-5-1471-2012, 2012.

Hakola, H., Tarvainen, V., Laurila, T., Hiltunen, V., Hellén, H. and Keronen, P.: Seasonal variation of VOC concentrations above a boreal coniferous forest. Atmospheric Environment, 37(12), 1623-1634, 2003.

Hallquist, M., Wenger, J. C., Baltensperger, U., Rudich, Y., Simpson, D., Claeys, M. and Dommen, J.: The formation , properties and impact of secondary organic aerosol : current and emerging issues, Atmos. Chem. Phys., 9, 5155–5236, 2009.

Halsey,G.: Physical adsorption on non-uniform surfaces, J. Chem. Phys., 16, 931–937, 1948.

Hilal, H., Karickhoff, S.W. and Carreira, L. A.: A Rigorous Test for SPARC's Chemical Reactivity Models: Estimation of More Than 4300 Ionization pKas. Quant. Struct.-Act. Relat., 14: 348–355. doi:10.1002/qsar.19950140405, 1995.

Hill, T.L.: Physical adsorption and the free volume model for liquids, J. Chem. Phys., 17, 590, 1949.

Hjellbrekke, A. G. and Fjæraa, A.M.: Data Report 2008 Acidifying and eutrophying compounds and particulate matter, Norwegian Institute for Air Research, Kjeller, EMEP/CCC-Report 1/2010, 2010.

Hodas, N., Zuend, A., Schilling, K., Berkemeier, T., Shiraiwa, M., Flagan, R.C. and Seinfeld, J.H.: Discontinuities in hygroscopic growth below and above water saturation for laboratory surrogates of oligomers in organic atmospheric aerosols, Atmos. Chem. Phys., 16, 12767-12792, doi:10.5194/acp-16-12767-2016, 2016.

Hu, W. W., Campuzano-Jost, P., Palm, B .B., Day, D. A., Ortega, A.M., Hayes, P. L., Krechmer, J. E., Chen, Q., Kuwata, M., Liu, Y. J., de Sá, S. S., McKinney, K., Martin, S. T., Hu, M., Budisulistiorini, S. H., Riva, M., Surratt, J. D., St. Clair, J. M., Isaacman-Van Wertz, G., Yee, L.D., Goldstein, D., A. H., Carbone, S., Brito, J., Artaxo, P., de Gouw, J. A., Koss, A., Wisthaler, A., Mikoviny, T., Karl, T., Kaser, L., Jud, W., Hansel, A., Docherty, K. S., Alexander, M. L., N. H. Robinson, N.H., Coe, H., Allan, J. D., Canagaratna, M. R., Paulot, F. and Jimenez, J. L.: Characterization of a real-time tracer for isoprene epoxydiols-derived secondary organic aerosol (IEPOX-SOA) from aerosol mass spectrometer measurements, Atmos. Chem. Phys., 15, 11807-11833, doi:10.5194/acp-15-11807-2015, 2015.

Huff-Hartz, K. E. H., Tischuk, J. E., Chan, M. N., Chan, C. K., Donahue, N. M., and Pandis, S. N.: Cloud condensation nuclei activation of limited solubility organic aerosol, Atmos. Environ., 40, 605–617, 2006.

Intergovernmental Panel on Climate Change (IPCC), Climate Change 2013: The Scientific Basis: Contribution of Working Group I to the Fifth Assessment Report of the Intergovernmental Panel on Climate Change, Cambridge Univ. Press, New York, 2013.

Iversen, T., Bentsen, M., Bethke, I., Debernard, J. B., Kirkevåg, A., Seland, Ø., Drange, H., Kristjansson, J. E., Medhaug, I., Sand, M. and Seierstad, I. A.: The Norwegian Earth System Model, NorESM1-M - Part 2: Climate response and scenario projections, Geosci. Model Dev., 6, 389-415, doi:10.5194/gmd-6-389-2013, 2013.

J. E. Jiusto, J.E. and Kocmond, W. C.: Condensation on nonhygroscopic particles, J. Rech. Atmos., 3, 19–24, 1968.

Jimenez, J. L., Canagaratna, M. R., Donahue, N. M., Prevot, a S. H., Zhang, Q., Kroll, J. H., DeCarlo, P. F., Allan, J. D., Coe, H., Ng, N. L., Aiken, a C.,

Docherty, K. S., Ulbrich, I. M., Grieshop, a P., Robinson, a L., Duplissy, J., Smith, J. D., Wilson, K. R., Lanz, V. a, Hueglin, C., Sun, Y. L., Tian, J., Laaksonen, a, Raatikainen, T., Rautiainen, J., Vaattovaara, P., Ehn, M., Kulmala, M., Tomlinson, J. M., Collins, D. R., Cubison, M. J., Dunlea, E. J., Huffman, J. a, Onasch, T. B., Alfarra, M. R., Williams, P. I., Bower, K., Kondo, Y., Schneider, J., Drewnick, F., Borrmann, S., Weimer, S., Demerjian, K., Salcedo, D., Cottrell, L., Griffin, R., Takami, a, Miyoshi, T., Hatakeyama, S., Shimono, a, Sun, J. Y., Zhang, Y. M., Dzepina, K., Kimmel, J.

Jokinen, V., and Makela, J. M.: Closed-loop arrangement with critical orifice for DMA sheath excess flow system, J Aerosol Sci, 28, 643-648, 1997.

Junge, C.: Das Wachstum der Kondensationskerne mit der relativen Feuchtigkeit. Ann. Meteor., 3, 129-135, 1950

Kaiser, J., Skog, K. M., Baumann, K., Bertman, S.B., Brown, S. B., Brune, W.H., Crounse, J. D., de Gouw, J. A., Edgerton, E.S., Feiner, P. F., Goldstein, A. H., Koss, A., Misztal, P. K., Nguyen, T. B., Olson, K. F., St. Clair, J. M., Teng, A. P., Toma, S., Wennberg, P. O., Wild, R. J., Zhang, L. and Keutsch, F. N. : Speciation of OH reactivity above the canopy of an isoprene-dominated forest, Atmos. Chem. Phys., 16, 9349-9359, doi:10.5194/acp-16-9349-2016, 2016.

Kanakidou, M., Seinfeld, J. H., Pandis, S. N., Barnes, I., Dentener, F. J., Facchini, M. C., Van Dingenen, R., Ervens, B., Nenes, a., Nielsen, C. J., Swietlicki, E., Putaud, J. P., Balkanski, Y., Fuzzi, S., Horth, J., Moortgat, G. K., Winterhalter, R., Myhre, C. E. L., Tsigaridis, K., Vignati, E., Stephanou, E. G. and Wilson, J.: Organic aerosol and global climate modelling: a review, Atmos. Chem. Phys., 5(4), 1053–1123, doi:10.5194/acp-5-1053-2005, 2005.

Kang, E., Root, M. J., Toohey, D. W. and Brune, W. H.: Introducing the concept of Potential Aerosol Mass (PAM), Atmos. Chem. Phys., 7, 5727-5744, 2007.

Kang, E., Root, M.J., Toohey, D.W. and Brune, W. H.: Introducing the concept of Potential Aerosol Mass (PAM), Atmos. Chem. Phys., 7, 5727-5744, 2007.

Kerker, M.: The scattering of light and other electromagnetic radiation. New York, London: Academic Press, 1969.

Kesselmeier, J. and Staudt, M: Biogenic volatile organic compounds (VOC): An overview on emission, physiology and ecology, Atmos. Chem, 33(1), 23-88, 1999.

Knutson, E. O., Whitby, K. T.: Anomalous unipolar diffusion charging of polystyrene latex aerosols. Journal of Colloid and Interface Science, 53, 493-495, 1975.

Kreidenweis, S. M., Petters, M. D., and DeMott, P. J.: Deliquescence-controlled activation of organic aerosols, Geophys. Res. Lett., 33, L06801, doi:10.1029/2005GL024863, 2006.

Krieger, U. K., Marcolli, C., Reid, J. P.: Exploring the complexity of aerosol particle properties and processes using single particle techniques, Chem. Soc. Rev., 41, 6631-6662, 2012.

Kroll, J. H., Donahue, N. M., Jimenez, J. L., Kessler, S. H., Canagaratna, M. R., Wilson, K. R., Altieri, K. E., Mazzoleni, L. R., Wozniak, A. S., Bluhm, H., Mysak, E. R., Smith, J. D., Kolb, C. E., Worsnop, D. R. Carbon oxidation state as a metric for describing the chemistry of atmospheric organic aerosol, Nature Chem., 3, 133-139, 2011.

Kumar, P., Sokolik, I. N. and Nenes, A.: Cloud condensation nuclei activity and droplet activation kinetics of wet processed regional dust samples and minerals. Atmos. Chem. and Phys., 11(16), 8661-8676, 2011a.

Kumar, P., Sokolik, I. N. and Nenes, A.: Measurements of cloud condensation nuclei activity and droplet activation kinetics of fresh unprocessed regional dust samples and minerals, Atmos. Chem. Phys., 11, 3527–3541, doi: 10.5194/acp-11-3527-2011, 2011b.

Kumar, P., Sokolik, I. N. and Nenes, A.: Parameterization of cloud droplet formation for global and regional models: including adsorption activation from insoluble CCN. Atmos. Chem. Phys., 9(7), 2517-2532, 2009.

Köhler, H.: The nucleus in and the growth of hygroscopic droplets, Trans Farad Soc, 32, 1152–1161, 1936.

Lambe, A., Onasch, T., Massoli, P., Croasdale, D., Wright, J., Ahern, A., Williams, L., Worsnop, D., Brune, W., and Davidovits, P.: Laboratory studies of the chemical composition and cloud condensation nuclei (CCN) activity of secondary organic aerosol (SOA) and oxidized primary organic aerosol (OPOA), Atmospheric Chemistry and Physics, 11, 8913-8928, 2011.

Lance, S., Nenes, A., Medina, J. and Smith, J.: Mapping the operation of the DMT continuous flow CCN counter, Aerosol Sci. Tech., 40(4), 242–254, doi:10.1080/02786820500432290, 2006.

Liu, P. F., Abdelmalki, N., Hung, H.M., Wang, Y., Brune, W. H. and Martin, S. T.: Ultraviolet and visible complex refractive indices of secondary organic material produced by photooxidation of the aromatic compounds toluene and m-xylene, Atmos. Chem. Phys., 15, 1435-1446, 10.5194/acp-15-1435-2015, 2015.

Liu, X., and Wang, J.: How important is organic aerosol hygroscopicity to aerosol indirect forcing? Environ. Res. Lett., 5(4), 044010, doi:10.1088/1748-9326/5/4/044010, 2010.

Liu, X., Cheng, Y., Zhang, Y., Jung, J., Sugimoto, N., Chang, S.-Y., Kim, Y. J., Fan, S. and Zeng, L.: Influences of relative humidity and particle chemical composition on aerosol scattering properties during the 2006 PRD campaign, Atmos. Environ., 42(7), 1525–1536, doi:10.1016/j.atmosenv.2007.10.077, 2008.

Lohmann, U. and Feichter, J.: Global indirect aerosol effects: a review, Atmos. Chem. Phys., 5, 715-737, https://doi.org/10.5194/acp-5-715-2005, 2005.

Lohmann, U. and Hoose, C.: Sensitivity studies of different aerosol indirect effects in mixed-phase clouds, Atmos. Chem. Phys., 9, 8917-8934, doi: 10.5194/acp-9-8917-2009, 2009.

McCartney, E. J.: Optics of the Atmosphere, John Wiley, New York, 1976.

McDonald, J.E.: Cloud nucleation on insoluble particle, J. Atmos. Sci., 21, 109–116, 1964.

McMurry, P. H. and Stolzenburg, M. R.: on the sensitivity of particle size to relative humidity for Los Angeles aerosols, Atmos. Environ, vol.23, 497-507, 1988.

Morales Betancourt, R. and Nenes, A.: Understanding the contributions of aerosol properties and parameterization discrepancies to droplet number variability in a global climate model. Atmospheric Chemistry and Physics, 14(9), 4809-4826, 2014.

Petters, M. D. and Kreidenweis, S. M.: A single parameter representation of hygroscopic growth and cloud condensation nucleus activity, Atmos. Chem. Phys., 7(8), 1961–1971, doi:10.5194/acp-7-1961-2007, 2007.

Petters, M. D., Wex, H., Carrico, C. M., Hallbauer, E., Massling, A., McMeeking, G. R., Poulain, L., Wu, Z., Kreidenweis, S. M., and Stratmann, F.: Towards closing the gap between hygroscopic growth and activation for secondary organic aerosol – Part 2: Theoretical approaches, Atmos. Chem. Phys., 9, 3999–4009, doi:10.5194/acp-9-3999-2009, 2009.

Prenni, A. J., Petters, M. D., Kreidenweis, S. M., DeMott, P. J. and Ziemann, P. J.: Cloud droplet activation of secondary organic aerosol, J. Geophys. Res., 112(D10), D10223, doi:10.1029/2006JD007963, 2007.

Psfai, M., Anderson, R. and Buseck, R.: Wet and dry sizes of atmospheric aerosol particles- An AFM-TEM study, , 25(11), 1907–1910, 1998.

Raatikainen, T., Vaattovaara, P., Tiitta, P., Miettinen, P., Rautiainen, J., Ehn, M., Kulmala, M., Laaksonen, A. and Worsnop, D. R.: Physicochemical properties and origin of organic groups detected in boreal forest using an aerosol mass spectrometer, Atmos. Chem. Phys., 10, 2063-2077, doi:10.5194/acp-10-2063-2010, 2010.

Raymond, T. M. and Pandis, S. N.: Cloud activation of single-component organic aerosol particles, J. Geophys. Res., 107(D24), 4787, doi: 10.1029/2002JD002159, 2002.

Renbaum-Wolff, L., Song, M., Marcolli, C., Zhang, Y., Liu, P.F., Grayson, J. W., Geiger, F.M., Martin, S. T. and Bertram, A.K.: Observations and implications of liquid–liquid phase separation at high relative humidities in secondary organic material produced by α-pinene ozonolysis without inorganic salts. Atmospheric Chemistry and Physics, 16(12), 7969-7979, 2016.

Ricchiazzi, P., Yang, S., Gautier, C., and Sowle, D.: SBDART: a research and teaching software tool for plane-parallel radiative transfer in the Earth's atmosphere, B. Am. Meteorol. Soc., 79, 2101–2114, 1998.

Roberts, C. G and Nenes, A.: A Continuous-Flow Streamwise Thermal-Gradient CCN Chamber for Atmospheric Measurements. Aerosol Sci. Technol., 39, 206–221, 2005.

Ruehl, C. R., Davies, J. F., Wilson, K. R.: An interfacial mechanism for cloud droplet formation on organic aerosols, Science, 351(6280), 1447-1450, 2016.

Saxena, P., Hildemann, L. M., McMurry, P. H. and Seinfeld, J. H.: Organics alter hygroscopic behavior of atmospheric particles, J. Geophys. Res. Atmos., 100(D9), 18755–18770, doi:10.1029/95JD01835, 1995.

Seinfeld, J. H. and Pandis, S. N.: Atmospheric Chemistry and Physics. Wiley, NewYork, 1998.

Serreze, M. C., Holland, M. M. and Stroeve, J.: Perspectives on the Arctic's shrinking sea-ice cover, Science, 315(5818), 1533–6, doi:10.1126/science.1139426, 2007.

Shindell, D. and Faluvegi, G.: Climate response to regional radiative forcing during the twentieth century. Nat. Geo., 2, 294-300, 2009.

Silvergren, S., Wideqvist, U., Ström, J., Sjogren, S. and Svenningsson, B.: Hygroscopic growth and cloud forming potential of Arctic aerosol based on observed chemical and physical characteristics (a 1 year study 2007-2008), J. Geophys. Res. Atmos., doi:10.1002/2014JD021657, 2014.

Song, M., Marcolli, C., Krieger, U. K., Zuend, A., Peter, T.: Liquid-liquid phase separation in aerosol particles: Dependence on O: C, organic functionalities, and compositional complexity, Geophys. Res. Lett., 39(19), 2012.

Sorjamaa, R. and Laaksonen, A.: The effect of H 2 O adsorption on cloud drop activation of insoluble particles: A theoretical framework. Atmos. Chem. and Phys., 7(24), 6175-6180, 2007.

Stevens, B., Giorgetta, M., Esch, M., Mauritsen, T., Crueger, T., Rast, S., Salzmann, M., Schmidt, H., Bader, J., Block, K., Brokopf, R., Fast, I., Kinne, S., Kornblueh, L., Lohmann, U., Pincus, R., Reichler, T. and Roeckner, E.: Atmospheric component of the MPI-M Earth System Model: ECHAM6, J. Adv. Model. Earth Syst., 5(2), 146-172, 2013.

Ström, J., Umegård, J., Tørseth, K., Tunved, P., Hansson, H.-C., Holmén, K., Wismann, V., Herber, a. and König-Langlo, G.: One year of particle size distribution and aerosol chemical composition measurements at the Zeppelin Station, Svalbard, March 2000–March 2001, Phys. Chem. Earth, Parts A/B/C, 28(28-32), 1181–1190, doi:10.1016/j.pce.2003.08.058, 2003.

Tang, I. N., Munkelwitz, H. R. and Davis, J. G.: aerosol growth studies - IV. phase transformation of mixed salt aerosols in a moist atmosphere, J. Aerosol Sci. Vol. 9, pp. 505-511, 1978.

Tang, I. N., Tridico, a. C. and Fung, K. H.: Thermodynamic and optical properties of sea salt aerosols, J. Geophys. Res., 102(D19), 23269, doi:10.1029/97JD01806, 1997.

Tang, I. N.: Phase transformation and growth of aerosol particles composed of mixed salts, J. Aerosol Sci., 7(5), 361–371, doi:10.1016/0021-8502(76)90022-7, 1976.

Topping, D. O. and McFiggans, G.: Tight coupling of particle size, number and composition in atmospheric cloud droplet activation, Atmos. Chem. Phys., 12, 3253–3260, doi:10.5194/acp-12-3253-2012, 2012.

Topping, D. O., Barley, M. H., McFiggans, G.: The sensitivity of Secondary Organic Aerosol component partitioning to the predictions of component properties–Part 2: Determination of particle hygroscopicity and its dependence on" apparent" volatility, Atmos. Chem. Phys., 11, 7767-7779, 2011.

Tsigaridis, K., Daskalakis, N., Kanakidou, M., Adams, P. J., Artaxo, P., Bahadur, R., Balkanski, Y., Bauer, S. E., Bellouin, N., Benedetti, A., Bergman, T., Berntsen, T.K., Beukes, J. P., Bian, H., Carslaw, K.S., Chin, M., Curci, G., Diehl, T., Easter, R.C., Ghan, S. J., Gong, S.L., Hodzic, A., Hoyle, C.R., Iversen, T., Jathar, S., Jimenez, J. L., Kaiser, J.W., Kirkevåg, A., Koch, D., Kokkola, H., Lee, Y. H., Lin, G., Liu, X., Luo, G., Ma, X., Mann, G.W., Mihalopoulos, N., Morcrette, J. J., Müller, J. F., Myhre, G., Myriokefalitakis, S., Ng, N. L., O'Donnell, D., Penner, J.E., Pozzoli, L., Pringle, K. J., Russell, L. M., Schulz, M., Sciare, J., Seland, Ø., Shindell, D. T., Sillman, S., Skeie, R. B., Spracklen, D., Stavrakou, T., Steenrod, S. D., Takemura, T., Tiitta, P., Tilmes, S., Tost, H., van Noije, T., van Zyl, P. G., von Salzen, K., Yu, F., Wang, Z., Wang, Z., Zaveri, R. A., Zhang, H., Zhang, K., Zhang, Q. and Zhang, X.: The AeroCom evaluation and intercomparison of organic aerosol in global models. Atmos. Chem. Phys., 14, 10845-10895, doi: 10.5194/acp-14-10845-2014, 2014.

Tunved, P., Strom, J., and Krejci, R.: Arctic aerosol life cycle: linking aerosol size distributions observed between 2000 and 2010 with air mass transport and precipitation at Zeppelin station, Ny-Alesund, Svalbard, Atmos. Chem. Phys., 13, 3643-3660, 10.5194/acp-13-3643-2013, 2013.

Twomey, S.: The Influence of Pollution on the Shortwave Albedo of Clouds, J. Atmos. Sci., 34(7), 1149–1152, doi:10.1175/1520-0469(1977)034<1149:TIOPOT>2.0.CO;2, 1977.

Van de Hulst, H. C.: Light Scattering By Small Particles, John Wiley & Sons, Inc., New York, 1957.

Vignati, E., Wilson, J. and Stier, P.: M7: An efficient size-resolved aerosol microphysics module for large-scale aerosol transport models, J. Geophys. Res., 109, D22202, doi:10.1029/2003JD004485, 2004.

Virkkula, A., Dingenen, R. Van, Raes, F. and Hjorth, J.: Hygroscopic properties of aerosol formed by oxidation of limonene , and lS-pinene, J. Geophys. Res, 104, 3569–3579, 1999.

Virtanen, A., Joutsensaari, J., Koop, T., Kannosto, J., Yli-Pirilä, P., Leskinen, J., Mäkelä, J.M., Holopainen, J. K., Pöschl, U., Kulmala, M., Worsnop, D.R. and Laaksonen, A.: An amorphous solid state of biogenic secondary organic aerosol particles. Nature, 467, 824–827, 2010.

Wallén, A., Lidén, G., and Hansson, H.-C.: Measured elemental carbon by thermo-optical transmittance analysis in water-soluble extracts from diesel exhaust, woodsmoke, and ambient particulate samples. J. Occup. Environ. Hyg.7 (1), 35-45, 2010.

Warneck, P.: Chemistry of the natural atmosphere, Academic Press, 1998.

Wex, H., Petters, M. D., Carrico, C. M., Hallbauer, E., Massling, A., McMeeking, G. R., Poulain, L., Wu, Z., Kreidenweis, S. M. and Stratmann, F.: Towards closing the gap between hygroscopic growth and activation for secondary organic aerosol: Part 1–Evidence from measurements. Atmos. Chem. and Phys., 9(12), 3987-3997, 2009.

Wiscombe, W.: Mie scattering calculations: Advances in technique and fast, vector-speed computer codes, NCAR Technical Note NCAR/TN-140+STR, available from National Technical Information Service as NTIS PB 301388, 1979.

Xu, L., Guo, H., Boyd, C. M., Klein, M., Bougiatioti, A., Cerully, K. M., Hite, J. R., Isaacman-VanWertz, G., Kreisberg, N. M., Knote, C., Olson, K., Koss, A., Goldstein, A., Hering, S. V., de Gouw, J., Baumann, K., Lee, S. H., Nenes, A., Weber, R. J. and Ng, N. L.: Effects of anthropogenic emissions on aerosol formation from isoprene and monoterpenes in the southeastern United States, P. Natl. Acad. Sci. USA, 112, 37–42, doi:10.1073/pnas.1512279112, 2015.

You, Y., Smith, M. L., Song, M., Martin, S.T. and Bertram, A. K.: Liquid–liquid phase separation in atmospherically relevant particles consisting of organic species and inorganic salts. Inter. Rev. Phys. Chem., 33(1), 43-77, 2014.

Zhang, K., O'Donnell, D., Kazil, J., Stier, P., Kinne, S., Lohmann, U., Ferrachat, S., Croft, B., Quaas, J., Wan, H., Rast, S. and Feichter, J.: The global aerosol-climate model ECHAM-HAM, version 2: sensitivity to improvements in process representations, Atmos. Chem. Phys., 12, 8911-8949, doi:10.5194/acp-12-8911-2012, 2012.

Zhang, Q., Jimenez, J. L., Canagaratna, M. R., Allan, J. D., Coe, H., Ulbrich, I., Alfarra, M. R., Takami, a., Middlebrook, a. M., Sun, Y. L., Dzepina, K., Dunlea, E., Docherty, K., DeCarlo, P. F., Salcedo, D., Onasch, T., Jayne, J. T., Miyoshi, T., Shimono, a., Hatakeyama, S., Takegawa, N., Kondo, Y., Schneider, J., Drewnick, F., Borrmann, S., Weimer, S., Demerjian, K., Williams, P., Bower, K., Bahreini, R., Cottrell, L., Griffin, R. J., Rautiainen, J., Sun, J. Y., Zhang, Y. M. and Worsnop, D. R.: Ubiquity and dominance of oxygenated species in organic aerosols in anthropogenically-influenced Northern Hemisphere midlatitudes, Geophys. Res. Lett., 34(13), L13801, doi:10.1029/2007GL029979, 2007.

Zieger, P., Fierz-Schmidhauser, R., Weingartner, E. and Baltensperger, U.: Effects of relative humidity on aerosol light scattering: results from different European sites, Atmos. Chem. Phys., 13(21), 10609–10631, doi:10.5194/acp-13-10609-2013, 2013.

Zieger, P., Wehrle, G., Jefferson, A., Ogren, J. A., Baltensperger, U. and Weingartner, E.: Measurement of relative humidity dependent light scattering of aerosols, Atmos. Chem. Phys, (1993), 39–50, 2010.

Zuend, A. and Seinfeld, J.H.: A practical method for the calculation of liquid–liquid equilibria in multicomponent organic–water–electrolyte systems using physicochemical constraints. Fluid Phase Equilibria, 337, 201-213, 2013.

Zuend, A. and Seinfeld, J.H.: Modeling the gas-particle partitioning of secondary organic aerosol: the importance of liquid-liquid phase separation. Atmos. Chem. Phys., 12(9), 3857-3882, 2012.